

Discovery of 3*H*-Benzo[4,5]thieno[3,2-*d*]pyrimidin-4-ones as Potent, Highly Selective, and Orally Bioavailable Inhibitors of the Human Protooncogene Proviral Insertion Site in Moloney Murine Leukemia Virus (PIM) Kinases

Zhi-Fu Tao,* Lisa A. Hasvold, Joel D. Levenson, Edward K. Han, Ran Guan, Eric F. Johnson, Vincent S. Stoll, Kent D. Stewart, Geoff Stamper, Nirupama Soni, Jennifer J. Bouska, Yan Luo, Thomas J. Sowin, Nan-Horng Lin, Vincent S. Giranda, Saul H. Rosenberg, and Thomas D. Penning

Cancer Research, Global Pharmaceutical Research and Development, Abbott Laboratories, Abbott Park, Illinois 60064

Received June 26, 2009

Pim-1, Pim-2, and Pim-3 are a family of serine/threonine kinases which have been found to be overexpressed in a variety of hematopoietic malignancies and solid tumors. Benzothienopyrimidinones were discovered as a novel class of Pim inhibitors that potently inhibit all three Pim kinases with subnanomolar to low single-digit nanomolar K_i values and exhibit excellent selectivity against a panel of diverse kinases. Protein crystal structures of the bound Pim-1 complexes of benzothienopyrimidinones **3b** (PDB code 3JYA), **6e** (PDB code 3JYO), and **12b** (PDB code 3JXW) were determined and used to guide SAR studies. Multiple compounds exhibited potent antiproliferative activity in K562 and MV4-11 cells with submicromolar EC_{50} values. For example, compound **14j** inhibited the growth of K562 cells with an EC_{50} value of 1.7 μ M and showed K_i values of 2, 3, and 0.5 nM against Pim-1, Pim-2, and Pim-3, respectively. These novel Pim kinase inhibitors efficiently interrupted the phosphorylation of Bad in both K562 and LnCaP-Bad cell lines, indicating that their potent biological activities are mechanism-based. The pharmacokinetics of **14j** was studied in CD-1 mice and shown to exhibit bioavailability of 76% after oral dosing. ADME profiling of **14j** suggested a long half-life in both human and mouse liver microsomes, good permeability, modest protein binding, and no CYP inhibition below 20 μ M concentration.

Introduction

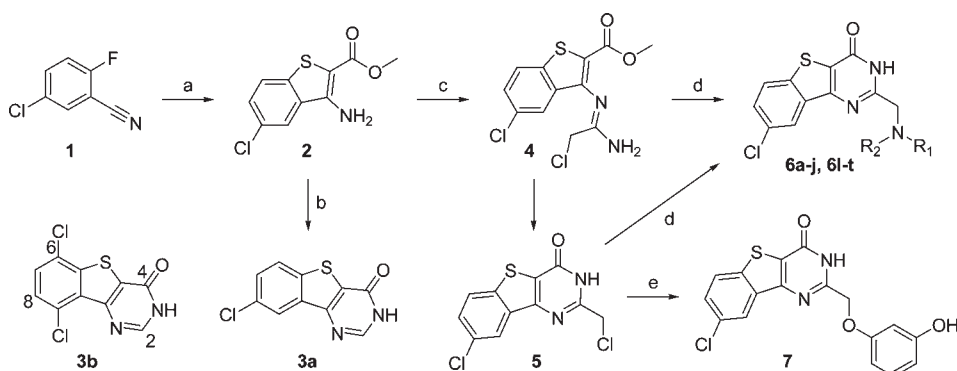
The Pim kinases are a family of three serine/threonine kinases, Pim-1, Pim-2, and Pim-3, which were first identified in a series of retroviral insertional mutagenesis studies in *c-myc*-induced murine lymphomas and named for the genomic site, Proviral Integration site of moloney Murine leukemia virus.^{1,2} The Pim kinases are favorable partners for *myc*-induced tumorigenesis and can play functionally important roles in this process.^{3–5} Pim-1/Pim-2/Pim-3 triple knockout mice are viable, but they are significantly smaller than their wild-type counterparts, clearly due to reduced cell proliferation.⁶ Pim kinases have been demonstrated to inhibit apoptosis by inducing antiapoptotic Bcl-2 expression or inactivating the pro-apoptotic protein Bad^a through phosphorylation.^{7–10} Pim-1 and Pim-2 have been found to be overexpressed in solid tumors such as prostate cancer^{11–13} and a variety of human hematopoietic malignancies^{14–16} such as leukemia and lymphoma. Pim kinases have been shown to be involved in the growth, survival, perineural invasion, and androgen independence of prostate cancer cells.^{17–19} Pim-3 is

overexpressed in human hepatoma cell lines and hepatocellular carcinoma tissues and has been shown to promote the growth of Ewing's family tumor cell lines.^{20,21a,b} More recently, Pim-3 was found to be aberrantly expressed in human colon and pancreatic cancers and to phosphorylate Bad, thereby blocking Bad-mediated apoptosis.^{21c,d} These findings suggest that small molecule inhibitors of Pim kinases may be of therapeutic value in the treatment of cancer.

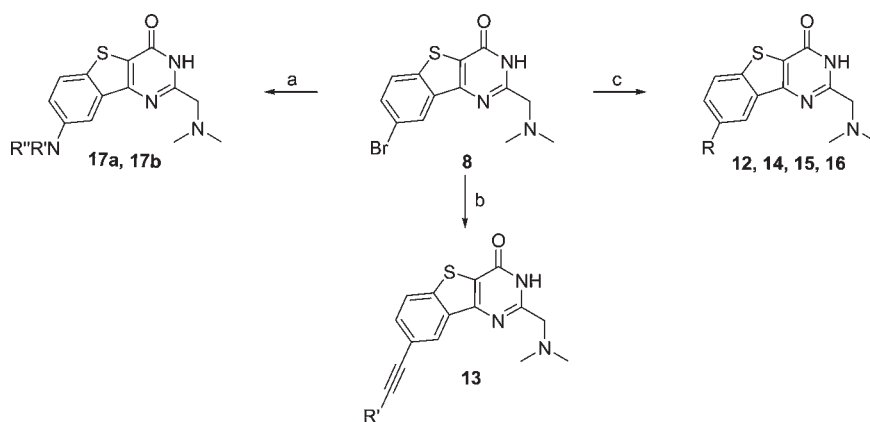
Several classes of Pim inhibitors have been reported recently, including ruthenium-containing organometallic complexes,^{22,23} bisindolylmaleimides,²⁴ imidazo[1,2-*b*]pyridazines,^{25–27} pyridones,²⁸ flavonoids,^{29,30} benzoisoxazoles,³¹ and isoxazoloquinoline-3,4(1*H*,9*H*)-diones.³² However, these molecules potentially inhibit only Pim-1, and the mechanism-based antitumor activity of the majority of these reported Pim-1 inhibitors remains to be described. Because all three Pim kinases have been implicated in tumorigenesis, it may be necessary to simultaneously target Pim-1, Pim-2, and Pim-3 to achieve optimal cancer therapy efficacy.^{33–35} Pim triple knockout mice are viable, suggesting that a favorable therapeutic window may be achieved for triple Pim-1, Pim-2, and Pim-3 inhibitors.⁶ Despite the high sequence conservation of the active sites for Pim-1 and Pim-2, it has been reported that Pim-2 is intrinsically more difficult to target.²⁵ During the preparation of this article, 5-arylidene-2,4-thiazolidinediones^{36a} and cinnamic acids^{36b} were reported to inhibit Pim-2. The most potent Pim-2 inhibitors based on thiazolidinedione and cinnamic acid have double-digit nanomolar IC_{50} values. The mechanism-based in vitro antitumor activity of the latter

*To whom correspondence should be addressed. Phone: (847)-938-6772. Fax: (847)-935-5165. E-mail: zhi-fu.tao@abbott.com.

^a Abbreviations: APCI, atmospheric pressure chemical ionization; ATP, adenosine-5'-triphosphate; BAD, Bcl-2 antagonist of cell death; DMF, *N,N*-dimethylformamide; DMSO, dimethyl sulfoxide; DTT, dithiothreitol; EDTA, ethylenediaminetetraacetic acid; HEPES, *N*-(2-hydroxyethyl)-piperazine-*N'*-2-ethanesulfonic acid; HTS, high-throughput screening; Pim, proviral insertion site in moloney murine leukemia virus; SAR, structure–activity relationship; THF, tetrahydrofuran.

Scheme 1^a

^a Reaction conditions: (a) 2-mercaptoacetate, aq NaOH, DMF, 0 °C, 95%; (b) formamide, 190 °C, 10 h, 13%; (c) HCl, 2-chloroacetonitrile, room temperature, quantitative yield; (d) amine, DMF, room temperature; (e) 1,3-dihydroxybenzene, K₂CO₃, DMF, 50 °C.

Scheme 2^a

^a Reaction conditions: (a) amines, biphenyl-2-yl-di-*tert*-butylphosphine, Pd₂(dba)₃, NaOtBu, toluene, microwave 120 °C; (b) Pd(PPh₃)₄, alkyne, DMF, microwave 100 °C; (c) boronic acids, Pd(PPh₃)₂Cl₂, microwave 160 °C, Na₂CO₃, DME/EtOH/H₂O.

remains to be disclosed.^{36b} To date, no potent Pim-3 inhibitor has been reported. We herein report that tricyclic benzothienopyrimidinones constitute a new class of Pim kinase inhibitors. On the basis of a HTS hit, medicinal chemistry efforts led to the identification of benzothienopyrimidinone-based Pim inhibitors that not only inhibit all three Pim kinases at subnanomolar to low single-digit nanomolar concentrations but also exhibit excellent kinase selectivity. Interestingly, this is the first time that a benzothienopyrimidinone scaffold has been used for kinase inhibition, which is in contrast to the fact that most other reported Pim inhibitors were developed based on known kinase inhibitor templates.

Chemistry

A general route for the synthesis of the 3*H*-benzo[4,5]thieno[3,2-*d*]pyrimidin-4-ones is shown in Scheme 1.³⁷ Fluorobenzonitriles **1** were condensed with methyl 2-mercaptoacetate and the resulting intermediates spontaneously cyclized to benzothiophene **2** under basic conditions in excellent yield. Compound **3a** was obtained through the condensation of **2** with formamide at high temperature. Compound **3b** was prepared by following a similar procedure used for the synthesis of **3a**. Compound **2** was reacted with chloroacetonitrile in 4 N HCl in dioxane to quantitatively provide the key intermediate **4**, which readily underwent cyclization under basic conditions to produce **5**. The chloromethyl group at the 2-position of **5** was an excellent handle for

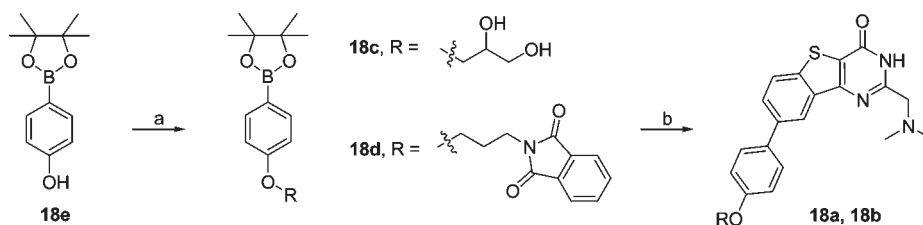
further elaboration, being readily displaced by nucleophilic amines and phenols. This simple alkylation expedited the synthesis of amine derivatives **6** and ether analogue **7** and thus greatly facilitated SAR studies.

Scheme 2 shows the synthesis of analogues derived from the 8-position of the phenyl ring. Compounds **8–11** were prepared by using the same route as shown in Scheme 1. Suzuki coupling of **8** with the corresponding boronic acid or boronic ester readily provided compounds **12** and **14–16**. Sonogashira reaction between **8** and various alkynes afforded compounds **13**. The amination of **8** was accomplished under Buchwald conditions to provide **17**. It is worth noting that all three Pd-mediated couplings were performed under microwave heating, which greatly shortened the reaction times.

Displayed in Scheme 3 is the synthesis of analogues **18a** and **18b** derived from compound **14j**. Advanced boronic esters **18c** and **18d** were obtained from the commercially available boronate **18e** through direct alkylation in moderate yields. Suzuki coupling under microwave conditions gave the desired products **18a** and **18b** in low to moderate yields.

Results and Discussion

Initial Hit from High-Throughput Screening (HTS). Compound **3b** was identified as a HTS hit which showed *K_i* values of 63 and 160 nM against Pim-1 and Pim-2, respectively. However, this compound also inhibited several other kinases (Table 5) such as Clk4 (*K_i* = 90 nM) and Pbk (*K_i* = 316 nM) and did not show

Scheme 3^a

^a Reaction conditions: (a) K_2CO_3 , DME, 20 h, 80 °C, 29–78%; (b) **8**, $\text{Pd}(\text{PPh}_3)_2\text{Cl}_2$, Na_2CO_3 , DME/EtOH/ H_2O (7:2:3), microwave 150 °C, 10 min, 20–34%.

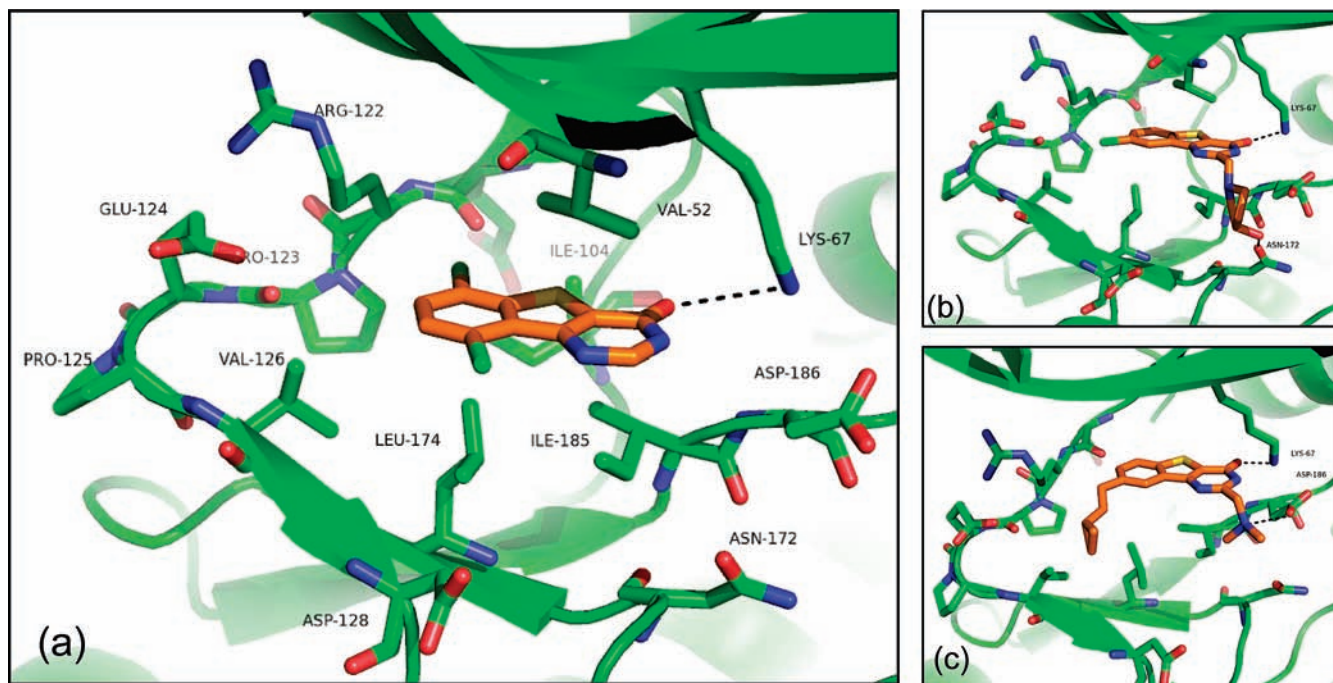


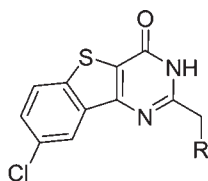
Figure 1. (a) X-ray crystal structure of compound **3b** (orange carbons) bound to Pim-1 kinase. A hydrogen bond with Lys67 is indicated with a black dotted line. (b,c) As in (a), with compounds **6e** and **12b**, respectively, with hydrogen bonds to Lys67 and Asn172/Asp186.

any cellular activity in multiple cell lines. The X-ray crystallographic analysis of a **3b**–Pim-1 complex indicated that the compound binds to the ATP-binding pocket (Figure 1a). The molecule is situated in the ATP-binding pocket in such a way that the phenyl ring interacts with the proline-containing hinge region, and the pyrimidone faces the pocket surrounded by Lys67, Glu89, and Phe49. The 2-position of the pyrimidone ring and the 8- and 9-positions of the phenyl ring are exposed to the solvent-accessible region, indicating that these positions should be able to accommodate a variety of substitutions to improve potency and adjust physicochemical properties. Due to the ready synthetic accessibility, we extensively investigated the SAR at the 2- and 8-positions based on **3a** (vide infra).

Structure–Activity Relationship at the 2-Position of the Pyrimidone Ring. A close examination of the X-ray structure of the **3b**–Pim-1 complex reveals that the 2-position of the pyrimidone ring points toward the solvent-exposed region through an area surrounded by Gly45, Phe49, Val52, Ile185, Asp186, Asn172, etc. Table 1 shows the SAR results at the 2-position. Polar residues such as Asp186 and Asn172 provide opportunities for basic amines to make polar interactions in this area. Therefore, we first introduced a series of aliphatic amines at the 2-position (**6a**–**6k**). The methylene linker between the amine nitrogen and the tricyclic core was expected to enhance the hydrophobic interaction with the

surrounding Gly45, Phe49, Val52, and/or Ile185. Although **3a** has slightly weaker affinity for Pim-1 and Pim-2 than the initial HTS hit **3b**, we chose to use **3a** as the starting point for this SAR exploration due to easier synthetic accessibility. The introduction of a simple dimethylaminomethyl group improved potency against Pim-1 and Pim-2 by 25- and 18-fold, respectively (**6a** vs **3a**). However, larger substituents such as piperidine (**6b**) and hexahydropyrimidine (**6c**) did not improve the potency. The elaboration of the dimethylamino group of **6a** by removing a methyl group (**6i**) or lengthening the methylene linker (**6j**, **6k**) did not increase the potency either. In contrast, the potency against Pim-2 was slightly decreased by these modifications. To explore possible H-bonding opportunities in this region, a hydroxyl group was incorporated into the substituents to provide compounds **6e**–**6h**. Gratifyingly, the hydroxylpyrrolidyl analogues (**6e**, **6f**) fully maintained the affinity for both Pim-1 and Pim-2 relative to **6a**, and the *S* configuration (**6e**) was identified as the better of the two. Aromatic groups were next introduced onto the 2-position (**6l**–**6t**). Substituents on the aryl ring of this set of analogues allowed probing of potential protein interactions with the Gly-rich loop and/or the side chains of Asp128/Glu171. Interestingly, the 3'-hydroxyl-phenyl analogue **6n** showed subnanomolar affinity to Pim-1, which is a 397-fold increase relative to **3a**. The Pim-2 inhibition

Table 1. SAR at the 2-Position of the Phenyl Ring



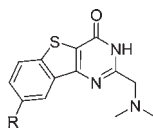
Compound	R	Pim-1 Inhibition (K_i , nM)	Pim-2 Inhibition (K_i , nM)
3a	H	358	1140
6a		14	63
6b		12	149
6c		11	138
6d		332	1250
6e		5	29
6f		9	84
6g		33	>1424
6h		42	206
6i		71	153
6j		17	399
6k		11	211
6l		44	> 1424

Compound	R	Pim-1 Inhibition (K_i , nM)	Pim-2 Inhibition (K_i , nM)
6m		92	>1424
6n		0.9	147
6o		107	> 1424
6p		92	> 1424
6q		66	711
6r		38	>1424
6s		18	>1424
6t		49	40
7		16	410

of **6n** was also improved 8-fold compared with **3a**. Unfortunately, other phenyl-containing analogues (**6m**, **6o–6t**) were significantly less potent than **6n**. Extension of the linker of **6n** modestly improved the affinity for Pim-2 at the expense of Pim-1 inhibition activity (**6t** vs **6n**). Replacement of the nitrogen linker with an oxygen considerably decreased the Pim-1 inhibition activity and modestly reduced the Pim-2 affinity (**6n** vs **7**). Finally, it should be noted that all substitutions at the 2-position significantly enhanced the affinity for Pim-1 compared with the parent compound **3a**, while the potency against Pim-2 varied significantly.

Structure–Activity Relationship at the 8-Position. The X-ray structure of the **3b**–Pim-1 complex indicates that the

8-position points toward the solvent front and is situated in a very hydrophobic area that is surrounded by Leu44, Ile104, Val126, and Leu174. To enhance hydrophobic interactions in this area, various lipophilic groups were installed at the 8-position (Table 2). Since the dimethylaminomethyl group was identified as one of the best groups at the 2-position, compound **9** was used as the starting point for the SAR studies at the 8-position. Compared with compound **9**, the introduction of a simple halogen atom (**6a**, **8**) or alkyl group (**10a**, **10b**, **11a**, **11b**) dramatically improved the affinity to both Pim-1 and Pim-2. The vinyl analogue **12a** is more potent than its saturated counterpart **11a**. The more hydrophobic cyclopropylvinyl group further increased the Pim-1

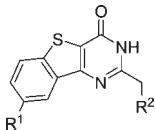
Table 2. SAR at the 8-Position of the Pyrimidinone Ring

Compound	R	Pim-1 Inhibition (K_i , nM)	Pim-2 Inhibition (K_i , nM)
6a	Cl	14	63
8	Br	5	16
9	H	296	238
10a	Me	32	122
10b	CF ₃	11	36
11a	Et	36	83
11b		20	21
12a		9	34
12b		1	2
13a		5	30
13b		40	99
13c		3	23
14a		4	8
14b		65	109
14c		6	13
14d		3	13
14e		5	44
14f		1	4
14g		14	32
14h		5	12
14i		5	21

and Pim-2 inhibition potency (**12b** vs **12a**). The acetylene analogue **13a** showed comparable activity to its alkene counterpart **12a**. However, the introduction of a polar dimethylamino group (**13b**) onto the acetylene terminus significantly decreased the Pim inhibition activity, consistent with the hydrophobicity of this area. Extending the methylene linker pushed the polar amino group into the solvent-exposed region and compound **13c** thereby regained high

Compound	R	Pim-1 Inhibition (K_i , nM)	Pim-2 Inhibition (K_i , nM)
14j		2	3
14k		2	2
14l		12	29
14m		1	5
14n		4	13
14o		8	22
14p		3	45
14q		4	>1420
15a		4	2
15b		8	3
15c		8	6
15d		11	7
16a		2	3
16b		29	66
17a		4	5
17b		271	120
18a		1	2
18b		0.6	6

Pim inhibition activity. Compounds **14a–14q** are phenyl-substituted analogues. Again, simple phenyl substitution at the 8-position considerably improved the Pim inhibition activity (**14a** vs **9**). Homologated analogue **14b** was less potent than **14a**, but was still much more active than the parent compound **9**. The *meta*-substituted phenyl analogues (**14c–14f**) maintained potency, and the 3'-hydroxyl-phenyl compound **14f** stood out as the most active analogue.

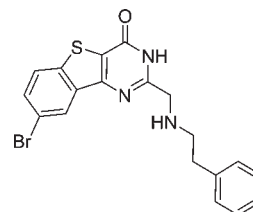
Table 3. K_i Values for Analogues Combining Optimal Substituents at the 2- and 8-Positions


Compound	R ¹	R ²	Pim-1 Inhibition (K_i , nM)	Pim-2 Inhibition (K_i , nM)
19a	Br		0.8	60
19b			2	152
19c	Ph		2	939
20a			5	3
20b	Ph		3	10
20c			0.7	2
20d			4	29
20e			0.8	0.9

An *ortho*-methyl-substitution negatively impacted activity (**14g** vs **14a**). Compounds **14h**–**14n** contain a *para*-substituted phenyl ring and showed relatively flat SAR. Molecular modeling indicated that the *para* substituent was situated in the solvent front, consistent with the flat SAR at this position. Compounds **14j** and **14k** showed superior activity for both Pim-1 and Pim-2, likely due to the solvation of the hydroxyl and amino groups at the *para* position. Further elaboration of the hydroxyl group of **14j** with solubilizing groups (**18a** and **18b**) fully retained the Pim inhibition activity and could potentially improve the physicochemical properties. The addition of a fluorine atom *ortho* to the hydroxyl group had little effect on inhibition of either Pim-1 or Pim-2 (**14m** vs **14j**). The 3',5'-disubstituted analogues fully maintained the inhibition activity to Pim-1 but lost significant Pim-2 activity (**14p** vs **14c**, **14q** vs **14d**). Analogues containing a five-membered aromatic ring (**15a**–**15c**) exhibited single-digit nanomolar K_i values for both Pim-1 and Pim-2. A methyl substituent on the thiophene ring slightly decreased activity (**15d** vs **15a**). The introduction of a nitrogen atom into the phenyl ring (**16a**) resulted in an increase of the affinity for both Pim-1 and Pim-2 (**16a** vs **14a**). However, the introduction of an additional nitrogen atom caused significant loss of activity (**16b** vs **14a**, **16b** vs **16a**), possibly due to an

Table 4. K_i Values for Pim-1, Pim-2, and Pim-3 for Select Compounds

compounds	Pim-1 inhibition (K_i , nM)	Pim-2 inhibition (K_i , nM)	Pim-3 inhibition (K_i , nM)
12b	1	2	0.2
14a	4	8	0.3
14d	3	13	0.7
14h	5	11	0.9
14i	5	21	1
14j	2	3	0.5
19a	8	60	4
20a	5	3	< 0.1
20b	3	10	0.3
20c	0.7	2	0.4
21	43	41	43

Chemical structure of compound **21**.

unfavorable contact between the second nitrogen and one of the hydrophobic amino acid residues in the extended hinge. Finally, selected saturated heterocycles were assessed (**17a**, **17b**), and it was found that the pyrrolidine ring is much more favorable at the 8-position than the piperidine ring (**17a** vs **17b**).

Compounds Combining the Optimal 2- and 8-Position Substituents. Table 3 shows compounds that combine some of the best substituents identified for the 2- and 8-positions. Compounds **19a**, **19b**, and **19c** all have the 3'-hydroxyphenylaminomethyl group at the 2-position and all showed low single-digit nanomolar potency against Pim-1 but much weaker affinity to Pim-2. The 3'-hydroxypyrrolidinyl group at the 2-position was then combined with various groups at the 8-position to provide compounds **20a**–**20e**. All of these compounds potently inhibit both Pim-1 and Pim-2. The results in Table 3 suggest that selective inhibitors against Pim-1 and dual inhibitors against both Pim-1 and Pim-2 can be readily obtained by fine-tuning the substitution at the 2-position, which will provide very useful tool compounds for elucidating the biological functions of Pim kinases.

Pim-3 Inhibition Activity. Pim-3 has been implicated in both human hematopoietic and malignant solid tumors.^{20,21} However, among the family of three serine/threonine Pim kinases, Pim-3 has received the least attention and no potent Pim-3 kinase inhibitors have been reported in the literature. We therefore set up a Pim-3 kinase enzymatic assay and tested a set of compounds from the tricyclic benzothienopyrimidinone series. As shown in Table 4, these compounds exhibited very high affinity for Pim-3. Notably, these compounds were usually more potent against Pim-3 than the other two Pim family kinases. The only exception was compound **21**, which was equipotent against all three Pim kinases.

X-ray Crystallographic Analysis and Molecular Modeling of the Inhibitor–Pim 1 Complexes. In order to guide the SAR studies and/or better understand the SAR results and binding mode, the X-ray crystallographic analysis of three compounds (**3b** (PDB code 3JYA), **6e** (PDB code 3JYO), and **12b** (PDB code 3JXW)) complexed with Pim-1 have been performed (Figure 1a–c).

The group of three Pim kinases is unique within the protein kinase family because of the presence of a proline residue (Pro123 in Pim-1) in the hinge, eliminating a key hydrogen-bond-donating hinge interaction to ATP and canonical kinase inhibitors.^{24,38} This leaves the backbone carbonyl of Glu121 as the sole hydrogen-bond-accepting partner available to ATP or inhibitors of Pim-1 kinase. There is also an additional proline (Pro 125) and a valine (Val 126) in the extended hinge, which provides a larger hydrophobic pocket for binding inhibitors. As shown in Figure 1a, the crystal structure of the screening hit, **3b**, exploits this novel hinge arrangement by placing a ring with two chlorine atoms nestled into the hydrophobic patch created by Pro123, the hydrophobic side chain of Arg122, Ile104 for one chlorine atom and the second more solvent-exposed in the direction of Val126. **3b** does not make any hydrogen bonds directly with the hinge. The sole hydrogen bond made by **3b** directly to the protein is between the inhibitor carbonyl and Lys67. The remainder of the inhibitor is sandwiched in the binding site in van der Waals contacts between Ile104, Ile185, and Leu174 on the bottom and the glycine-rich loop on the top.

The binding mode of **6e** (Figure 1b) has only a single chlorine atom pointed toward the extended hinge and has a slightly altered binding mode from **3b**. This shifts the single chlorine atom from the corresponding position observed in **3b** such that the remaining chlorine is in van der Waals contact with the hydrophobic portion of Arg122, Pro123, Val126, and Leu174. The carbonyl and the 3-N of the pyrimidine ring of **6e** form bidentate H-bonds with Lys67. The core of **6e** slightly shifts in upon removal of one chlorine relative to **3b**. Extension of a basic amine off the core demonstrates a significant improvement in potency, and this is most likely a result of electrostatic interaction with Asp186, although there is no formal hydrogen bonding observed. Interestingly, there is not a significant potency gain by adding a tertiary alcohol, which is observed in good hydrogen bonding distance to Asn172. This may be because this hydrogen bond is fairly solvent-exposed, thereby limiting its value.

The binding mode of **12b** (Figure 1c) is essentially identical to the monochloro compound, **6e**; however, **12b** is significantly more potent than **6e**. The binding modes of **12b** and **6e** are preserved relative to **3b** because the cyclopropyl extension on **12b** mimics and extends on the chlorine interactions of **6e**. The cyclopropyl extension contributes to a highly potent molecule for Pim-1 because it increases the van der Waals interactions with the extended hinge residues, Val126 in particular, as well as the hydrophobic portion of Arg122 and displacing water from the binding site. **12b** makes the same carbonyl and 3-N bidentate hydrogen bonds to Lys62 as **6e**. **12b** also extends a tertiary amine forming a hydrogen bond with Asp186, which has been demonstrated to significantly improve affinity. Combining all of these features, exploitation of the hydrophobic extended hinge, hydrogen bonding to Lys62, and electrostatic interaction with Asp186, results in the most potent analogue in this series for Pim-1.

In Tables 1 and 2 are shown the potencies for both Pim-1 and Pim-2 inhibition. In general, the compounds are more potent against Pim-1, but there are several analogues where there is equivalent activity. Active site differences within the Pim family are located within the hinge region at residues Glu124 and Val126 of Pim-1, which are Leu, Ala in Pim-2 and Glu, Ala in Pim-3, respectively. The electrostatic difference between Glu and Leu at position 124 would influence

Table 5. Kinase Selectivity of Pim Kinase Inhibitors

kinase	3b (K_i , μM) ^a	20c (K_i , μM)
Pim-1	0.1301	0.0007
Pim-2	0.1642	0.0021
Pim-3	0.0110	0.0004
BTk	0.6365	> 1
CDK2	> 1	> 1
CLK4	0.0896	> 1
EMK	> 1	> 1
IGF1R	0.9909	> 1
IRAK4	> 1	> 1
MSK1	0.7285	> 1
Map4k4	0.8124	> 1
P70S6K	0.7734	> 1
PBK	0.3161	> 1
PKA	> 1	> 1
PRKX	0.5847	> 1
Syk	0.3514	> 1
Src	> 1	> 1
TrkC	0.8283	> 1

^a The inhibition constant (K_i) values are calculated from the Cheng–Prusoff equation, $K_i = \text{IC}_{50}/(1 + ([\text{ATP}]/K_m))$.

desolvation during inhibitor binding, and the change between Val and Ala at 126 could influence steric and van der Waals contacts near the 8-position of the analogues. There are no residue differences in the Pim family in the immediate protein region of the 2-position of the analogues, so it is less clear why there is potency variation from probing that region.

Kinase Selectivity Profiles of Representative Pim Inhibitors. Two Pim kinase inhibitors (**3b**, **20c**) were tested for selectivity against other kinases. Compound **20c** is among the most potent compounds in the enzymatic assays against all three Pim kinases. Both compounds displayed remarkable selectivity against a panel of diverse kinases (Table 5). The initial HTS hit **3b** showed weak affinity for several other kinases. As discussed above, the crystal structure of **3b** provides a rationale for the Pim activity by showing that the chlorophenyl group occupies a hydrophobic region near the hinge provided by a proline residue (Pro123 in Pim-1). This hydrophobic interaction would not be present in non-Pim kinases because they do not have proline at this position and possess a H-bond donor from the backbone amide—the common kinase “hinge” pattern described for many other kinases. Therefore, a polarity clash with the chlorophenyl group of **3b** would make the observed binding mode in Pim-1 disfavored in other kinases. Alternatively, it is conceivable that simple, unsubstituted benzothienopyrimidinones, such as **3b**, could flip in the active site and present a canonical H-bond donor–acceptor interaction with the hinge using the pyrimidinone ring system, thus permitting weak activity on other kinases. However, the highly optimized analogues reported here with large substituents at positions 2 and 8 of the ring system would make this flipped binding mode less likely with concomitant enhanced kinome selectivity. The selectivity of lead compound **20c** was much improved compared with **3b**, exhibiting no inhibitory activity toward the other panel kinases even at the highest concentration tested (10 μM). With over 500 kinases in total, it has been very challenging for kinase-targeting drug discovery programs to achieve high selectivity.³⁹ Thus, the high kinase selectivity of the lead compound **20c** is truly impressive.

Cell-Based Assays of Select Pim Inhibitors. Select compounds with potent Pim-1 enzymatic activity in the enzymatic assay were further characterized for their antiproliferative

activity in K562 cells, a human leukemia cell line that over-expresses the Pim kinases. As shown in Table 6, multiple compounds potently killed these cancer cells and have sub-micromolar to low single-digit micromolar EC_{50} values. The K562 cell line has been reported to be resistant to Pim-1 selective inhibitors,²⁵ suggesting that Pim-2 inhibition may contribute significantly to the excellent cytotoxicity of these compounds against this cell line. The lack of a perfect correlation between Pim enzymatic inhibition potency and cellular antiproliferative activity may be due to physico-chemical properties such as variation in cellular penetration (for examples, please see ref 40), but our data did show a general trend that compounds with weak Pim-2 inhibition activity exhibit no antiproliferative activity in the K562 cell lines (e.g., **14i** and **20d**). These compounds were also evaluated in MV4-11, another human leukemia cell line, and all showed potent antiproliferative activity with EC_{50} values in the submicromolar to low single-digit micromolar range.

Table 6. Anti-proliferative Activities of Select Pim Inhibitors in K562 and MV4-11 Cell Lines

compounds	14f	14i	14j	14m	15b	18a	18b	20b	20c	20d
K562 (EC_{50} , μ M)	0.3	>30	1.7	6.1	0.7	4.7	5.9	0.4	1.4	>30
MV4-11 (EC_{50} , μ M)	1.4	4.1	2.4	3.2	1.9	0.8	1.5	5.6	1.3	2.7

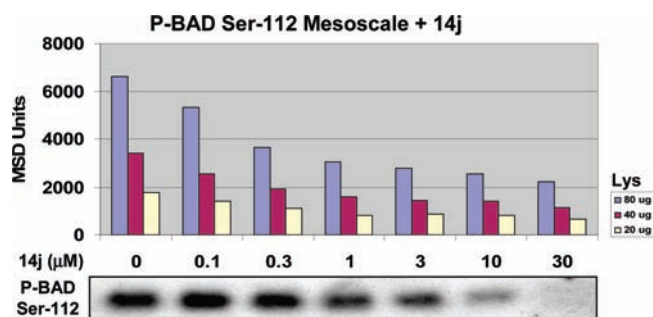


Figure 2. Compound **14j** inhibits the phosphorylation of Bad at serine-112. K562 cells were treated for 4 h with increasing concentrations of compound **14j**. Cell lysates were then analyzed by immunoblotting using an antibody directed against phospho-Bad serine-112.

Table 7. EC_{50} Values for the Inhibition of the Phosphorylation of Bad at Ser112 by Pim Inhibitors in the K562 and LnCaP-Bad Cell Lines

compounds	14f	14j	14m	20c	20e
K562 (EC_{50} , μ M)	0.5	0.5	0.35	0.4	0.15
LnCaP-Bad (EC_{50} , μ M)	NT ^a	NT	0.6	NT	0.7

^a Not tested.

Table 8. Pharmacokinetic Properties of Compound **14j**

	IV ^{a,b}				PO ^{a,c}			
	AUC (μ mol·h/L)	Cl (L/h/kg)	V_d (L/kg)	$t_{1/2}$ (h)	AUC (μ mol·h/L)	C_{max} (μ M)	T_{max} (h)	F (%)
14j	1.10	7.80	23.5	2.10	2.80	0.52	0.3	76

^a Three animals were used for each dosing group, and all values presented here were the averages of three animals. ^b The IV dosage was 3 mg/kg. ^c The oral dosage was 10 mg/kg.

Table 9. ADME Data for Compound **14j**

mouse liver microsomes ($t_{1/2}$, min)	human liver microsomes ($t_{1/2}$, min)	CYP (2C9, 2D6, 3A4) (IC_{50} , μ M)	Pampa (pH 7.4, % transported)	protein binding in 10% human plasma (% bound)	protein binding in 100% human plasma (% bound)
48	>60	>20	17.4	68	92

To further establish that the cytotoxicity of the benzothienopyrimidinone-based Pim inhibitors truly resulted from the inhibition of Pim kinases, we examined the phosphorylation of the pro-apoptotic protein Bad by Pim kinases in the presence or absence of Pim inhibitors in representative leukemia and prostate cancer cell lines. Bad, a downstream target of the Pim kinases, has been demonstrated to be directly phosphorylated at Ser112 and Ser136 by Pim-1, Pim-2, and Pim-3. It was found that these Pim inhibitors efficiently and dose-dependently inhibited the phosphorylation of Bad at Ser112 in K562 cells (Figure 2 and Table 7). In addition, the inhibition of Bad phosphorylation by two Pim inhibitors was tested in LnCaP prostate carcinoma cells engineered to express high levels of Bad (LnCaP-Bad).⁴¹ Compounds **14m** and **20e** both inhibited Bad phosphorylation with submicromolar EC_{50} values. These results strongly indicate that the benzothienopyrimidinone-based Pim inhibitors exert their cytotoxic effects through the inhibition of Pim kinases in cancer cells.

Pharmacokinetics of a Representative Pim Inhibitor. Since compound **14j** exhibited good overall activity in both enzymatic and cell-based assays, it was further characterized by evaluation of pharmacokinetics (PK). The compound was dosed into CD-1 mice with IV and oral administration. Compound **14j** is highly bioavailable and exhibited a bioavailability of 76% with oral dosing (Table 8). This compound showed a half-life of 2.1 h with IV dosing. Compound **14j** was further profiled for its ADME properties (Table 9). The compound was found to have good permeability, modest protein binding, a long half-life in both human and mouse liver microsomes, and no CYP inhibition below 20 μ M concentration.

Conclusions

We have discovered benzothienopyrimidinones as a novel class of Pim inhibitors. These new Pim inhibitors potently inhibit all three Pim kinases with K_i values ranging from subnanomolar to low single-digit nanomolar and exhibit excellent kinase selectivity against a panel of diverse kinases. More importantly, multiple compounds exhibited potent antiproliferative activity in K562 and MV4-11 cells with submicromolar EC_{50} values. The crystallographic structures of compounds **3b**, **6e**, and **12b** guided the SAR studies and will continue to play an important role in the further elaboration of this class of Pim inhibitors. These novel Pim inhibitors efficiently interrupted the phosphorylation of Bad in both K562 and LnCaP-Bad cell lines, supporting that their potent biological activities are mechanism-based. PK studies of a

representative compound (**14j**) suggested that these Pim inhibitors are highly bioavailable. To the best of our knowledge, these are the first examples of Pim inhibitors that simultaneously inhibit all three Pim kinases. They not only have great potential to be developed as medically useful agents but also have the potential to serve as powerful tools in the study of Pim-involved biological processes in cancer biology and immunology.⁴²

Experimental Section

General Information. All reactions were carried out under N₂ atmosphere unless otherwise specified. Reagents and solvents were obtained from commercial suppliers and were used without further purification. ¹H NMR spectra were obtained on a Varian UNITY or Inova (500 MHz), Varian UNITY (400 MHz), or Varian UNITY plus or Mercury (300 MHz) instrument. Chemical shifts are reported as δ values (ppm) downfield relative to TMS as an internal standard with multiplicities reported in the usual manner. Mass spectral analyses were performed on a Finnigan SSQ7000 GC/MS mass spectrometer using different techniques, including electrospray ionization (ESI), and atmospheric pressure chemical ionization (APCI), as specified for individual compounds. Exact mass measurements were performed on a Finnigan FTMS Newstar T70 mass spectrometer. The compound is determined to be "consistent" with the chemical formula if the exact mass measurement is within 5.0 ppm relative mass error (RME) of the exact monoisotopic mass. Elemental analyses were performed by Quantitative Technologies, Inc., Whitehouse, NJ. Column chromatography was carried out on a Horizon Pioneer system (Biotage, Inc.).

Preparative reverse-phase HPLC was performed on an automated Gilson HPLC system, using a SymmetryPrep Shield RP18 prep cartridge, 250 mm \times 21.20 mm i.d., 10 μ m, and a flow rate of 15 mL/min; λ = 214, 245 nm; mobile phase A, 0.1% TFA in H₂O; mobile phase B, CH₃CN; linear gradient 0–70% of B in 40 min.

Analytical LCMS with two different solvent systems (Methods A and B) indicated that the purity of all compounds was not less than 95%. Analytical LCMS was performed on a Finnigan Navigator mass spectrometer and Agilent 1100 HPLC system running Xcalibur 1.2 and Open-Access 1.3 software. The mass spectrometer was operated under positive APCI ionization conditions. The HPLC system comprised an Agilent Quaternary pump, degasser, column compartment, autosampler, and diode-array detector, with a Sedere Sedex 75 evaporative light-scattering detector. The column used was a Phenomenex Luna Combi-HTS C8(2) 5 μ m 100 Å (2.1 mm \times 30 mm). TFA Method (Method A): A gradient of 10–100% acetonitrile (solvent 1) and 0.1% trifluoroacetic acid in water (solvent 2) was used, at a flow rate of 2 mL/min (0–0.1 min 10% solvent 1, 0.1–2.6 min 10–100% solvent 1, 2.6–2.9 min 100–10% solvent 1, 2.9–3.0 min 100–10% solvent 1). Ammonium Method (Method B): A gradient of 10–100% acetonitrile (solvent 1) and 10 mM NH₄OAc in water (solvent 2) was used, at a flow rate of 1.5 mL/min (0–0.1 min 10% solvent 1, 0.1–3.1 min 10–100% solvent 1, 3.1–3.9 min 100–10% solvent 1, 3.9–4.0 min 100–10% solvent 1).

3-Amino-5-chlorobenzo[*b*]thiophene-2-carboxylic acid methyl ester (2**).** To a cold solution of 5-chloro-2-fluorobenzonitrile (10.5 g, 67.5 mmol) in DMF at 0 °C was dropwise added methyl 2-mercaptoacetate (6.45 mL, 70.88 mmol). The reaction mixture was stirred at 0 °C for 30 min, and then 5 M NaOH aqueous solution (20.25 mL) was added dropwise. After stirring at 0 °C for 3 h, the reaction mixture was quenched with ice–water. The resulting precipitate was collected by filtration and dried to give 15.4 g of white solid in 95% yield: MS (APCI) m/z 242 (M + H)⁺; ¹H NMR (300 MHz, DMSO-*d*₆) δ ppm 3.79 (s, 3 H), 7.18

(s, 2 H), 7.54 (dd, J = 8.82, 2.03 Hz, 1 H), 7.89 (d, J = 8.82 Hz, 1 H), 8.31 (d, J = 2.03 Hz, 1 H).

8-Chloro[1]benzothieno[3,2-*d*]pyrimidin-4(3*H*)-one (3a**).** **2** (242 mg, 1.0 mmol) was treated with formamide (8 mL, 0.2 mol) and heated at 190 °C for 6 h. The reaction mixture was cooled to room temperature and diluted with DMSO (2 mL). The resulting mixture was partitioned between ethyl acetate and water. The organic layer was washed with water (3 \times 50 mL) and brine, dried (MgSO₄), filtered, and concentrated. The concentrate was triturated with MeOH and filtered to collect the solid. The solid was further purified by reverse-phase preparative HPLC to provide the title compound (12.8 mg, 5% yield): MS (ESI) m/z 237 (M + H)⁺; ¹H NMR (300 MHz, DMSO-*d*₆) δ ppm 7.72 (dd, J = 8.65, 2.20 Hz, 1 H), 8.19–8.26 (m, 2 H), 8.37 (s, 1 H), 12.92 (s, 1 H).

5-Chloro-3-[(2-chloroacetimidoyl)amino]benzo[*b*]thiophene-2-carboxylic acid methyl ester (4**).** A suspension of **2** (6.2 g, 25.7 mmol) in 4 N hydrochloric acid in dioxane (70 mL) was treated with 2-chloroacetonitrile (3.18 mL, 50.32 mmol) at room temperature for 3 h. The white solid was collected by filtration and dried to give the desired product as the HCl salt quantitatively. The material was used directly in the next step without further purification: MS (APCI) m/z 317 (M + H)⁺.

8-Chloro-2-dimethylaminomethyl-3*H*-benzo[4,5]thieno[3,2-*d*]pyrimidin-4-one (6a**).** A mixture of **4** (30 mg, 0.076 mmol) and 2 M dimethylamine in methanol (2 mL) was stirred at room temperature overnight and concentrated. The residue was purified by reverse-phase preparative HPLC to provide the title compound in 56% yield: LCMS (APCI) m/z 294 (M + H)⁺; ¹H NMR (400 MHz, DMSO-*d*₆) δ ppm 3.04 (s, 6 H), 4.50 (s, 2 H), 7.73–7.78 (m, 1 H), 8.27 (d, J = 8.59 Hz, 1 H), 8.37 (d, J = 1.53 Hz, 1 H), 9.91 (br s, 1 H), 13.26 (br s, 1 H).

Compounds **6b–6t** were prepared by using a similar procedure described for the synthesis of **6a**.

8-Chloro-2-(piperidin-1-ylmethyl)[1]benzothieno[3,2-*d*]pyrimidin-4(3*H*)-one (6b**):** LCMS (APCI) m/z 334 (M + H)⁺; ¹H NMR (500 MHz, methanol-*d*₄) δ ppm 1.63–1.90 (m, 2 H), 1.89–2.10 (m, 4 H), 3.16–3.39 (m, 4 H), 4.51 (s, 2 H), 7.66 (dd, J = 8.54, 2.14 Hz, 1 H), 8.05 (d, J = 8.85 Hz, 1 H), 8.34 (d, J = 2.14 Hz, 1 H).

8-Chloro-2-(tetrahydropyrimidin-1(2*H*)-ylmethyl)[1]benzothieno[3,2-*d*]pyrimidin-4(3*H*)-one (6c**):** LCMS (APCI) m/z 335 (M + H)⁺; ¹H NMR (500 MHz, DMSO-*d*₆) δ ppm 1.80–2.01 (m, 2 H), 2.66–2.85 (m, 2 H), 3.07–3.15 (m, 2 H), 3.22–3.30 (m, 2 H), 4.36 (s, 2 H), 7.77 (dd, J = 8.70, 2.29 Hz, 1 H), 8.28 (d, J = 8.85 Hz, 1 H), 8.32 (d, J = 2.14 Hz, 1 H), 8.53 (s, 1 H), 8.75 (s, 1 H), 9.40 (s, 1 H), 13.24 (s, 1 H).

8-Chloro-2-(morpholin-4-ylmethyl)[1]benzothieno[3,2-*d*]pyrimidin-4(3*H*)-one (6d**):** LCMS (APCI) m/z 336 (M + H)⁺; ¹H NMR (500 MHz, methanol-*d*₄) δ ppm 3.37–3.50 (m, 4 H), 4.00 (t, J = 4.58 Hz, 4 H), 4.40 (s, 2 H), 7.66 (dd, J = 8.85, 2.14 Hz, 1 H), 8.05 (d, J = 8.54 Hz, 1 H), 8.35 (d, J = 2.14 Hz, 1 H).

8-Chloro-2-[(3*S*)-3-hydroxypyrrolidin-1-yl]methyl[1]benzothieno[3,2-*d*]pyrimidin-4(3*H*)-one (6e**):** LCMS (APCI) m/z 336 (M + H)⁺; ¹H NMR (400 MHz, methanol-*d*₄) δ ppm 2.13–2.28 (m, 1 H), 2.35 (br s, 1 H), 3.23–3.37 (m, 3 H), 3.81 (br s, 2 H), 4.64–4.69 (m, 1 H), 4.71 (s, 2 H), 7.65 (dd, J = 8.90, 2.15 Hz, 1 H), 8.04 (d, J = 8.29 Hz, 1 H), 8.38 (d, J = 2.15 Hz, 1 H); ¹H NMR (500 MHz, pyridine-*d*₅) δ ppm 2.03–2.15 (m, 1 H), 2.18–2.33 (m, 1 H), 3.00–3.12 (m, 1 H), 3.24–3.33 (m, 2 H), 3.33–3.42 (m, 1 H), 4.27–4.46 (m, 2 H), 4.64–4.79 (m, 1 H), 7.57 (dd, J = 8.85, 2.14 Hz, 1 H), 7.95 (d, J = 8.85 Hz, 1 H), 8.46 (d, J = 2.14 Hz, 1 H).

8-Chloro-2-[(3*R*)-3-hydroxypyrrolidin-1-yl]methyl[1]benzothieno[3,2-*d*]pyrimidin-4(3*H*)-one (6f**):** LCMS (APCI) m/z 336 (M + H)⁺; ¹H NMR (500 MHz, pyridine-*d*₅) δ ppm 2.01–2.12 (m, 1 H), 2.16–2.29 (m, 1 H), 2.92–3.04 (m, 1 H), 3.20–3.27 (m, 2 H), 3.27–3.35 (m, 1 H), 4.15–4.41 (m, 1 H), 4.56–4.83 (m, 1 H), 7.57 (dd, J = 2.14 Hz, 1 H), 7.95 (dd, J = 8.85, 2.14 Hz, 1 H), 8.47 (d, J = 2.14 Hz, 1 H).

8-Chloro-2-[(3-hydroxypiperidin-1-yl)methyl][1]benzothieno[3,2-*d*]pyrimidin-4(3*H*)-one (6g): LCMS (APCI) m/z 350 ($M + H$)⁺; ¹H NMR (500 MHz, DMSO-*d*₆) δ ppm 1.18–2.26 (m, 5 H), 3.31 (s, 2 H), 3.97 (s, 2 H), 4.41 (s, 2 H), 5.55 (s, 1 H), 7.76 (dd, $J = 8.70, 2.29$ Hz, 1 H), 8.27 (d, $J = 8.54$ Hz, 1 H), 8.31 (d, $J = 1.83$ Hz, 1 H), 9.26–10.27 (m, 1 H), 13.20 (s, 1 H).

8-Chloro-2-[(4-hydroxypiperidin-1-yl)methyl][1]benzothieno[3,2-*d*]pyrimidin-4(3*H*)-one (6h): LCMS (APCI) m/z 350 ($M + H$)⁺; ¹H NMR (500 MHz, DMSO-*d*₆) δ ppm 1.78 (br s, 2 H), 2.01 (br s, 2 H), 3.26 (br s, 2 H), 3.68 (br s, 2 H), 4.46 (br s, 2 H), 5.06 (br s, 1 H), 7.76 (dd, $J = 8.70, 2.29$ Hz, 1 H), 8.28 (d, $J = 8.54$ Hz, 1 H), 8.31 (d, $J = 2.14$ Hz, 1 H), 9.83 (br s, 1 H), 13.22 (br s, 1 H).

8-Chloro-2-[(methylamino)methyl][1]benzothieno[3,2-*d*]pyrimidin-4(3*H*)-one (6i): LCMS (APCI) m/z 280 ($M + H$)⁺; ¹H NMR (500 MHz, DMSO-*d*₆) δ ppm 2.79 (s, 3 H), 4.33 (s, 2 H), 7.76 (dd, $J = 8.54, 2.14$ Hz, 1 H), 8.27 (d, $J = 8.54$ Hz, 1 H), 8.35 (d, $J = 2.14$ Hz, 1 H), 9.29 (br s, 1 H).

8-Chloro-2-[2-(dimethylamino)ethyl][1]benzothieno[3,2-*d*]pyrimidin-4(3*H*)-one (6j): LCMS (APCI) m/z 308 ($M + H$)⁺; ¹H NMR (500 MHz, DMSO-*d*₆) δ ppm 2.91 (d, $J = 2.44$ Hz, 6 H), 3.21 (t, $J = 6.87$ Hz, 2 H), 3.65 (d, $J = 3.66$ Hz, 2 H), 7.73 (dd, $J = 8.70, 2.29$ Hz, 1 H), 8.24 (d, $J = 8.85$ Hz, 1 H), 8.30 (d, $J = 2.14$ Hz, 1 H), 9.28 (s, 1 H), 12.99 (s, 1 H).

8-Chloro-2-[3-(dimethylamino)propyl][1]benzothieno[3,2-*d*]pyrimidin-4(3*H*)-one (6k): A suspension of **2** (30 mg, 0.12 mmol) in 4 N hydrochloric acid in dioxane (10 mL) was treated with 4-aminobutanenitrile (101 mg, 1.2 mmol) at ambient temperature for 3 days. The reaction mixture was concentrated, and the residue was dissolved in DMF (1 mL). The resulting mixture was treated with 2 M dimethylamine in methanol (5 mL) at 50 °C overnight and concentrated. The residue was purified by HPLC to give the desired product: LCMS (APCI) m/z 322 ($M + H$)⁺; ¹H NMR (400 MHz, methanol-*d*₄) δ ppm 2.29–2.41 (m, 2 H), 2.93 (t, $J = 7.21$ Hz, 2 H), 2.97 (s, 6 H), 3.29–3.36 (m, 2 H), 7.60 (dd, $J = 8.59, 2.15$ Hz, 1 H), 7.98 (d, $J = 8.59$ Hz, 1 H), 8.24 (d, $J = 2.15$ Hz, 1 H).

2-(Anilinomethyl)-8-chloro[1]benzothieno[3,2-*d*]pyrimidin-4(3*H*)-one (6l): LCMS (APCI) m/z 342 ($M + H$)⁺; ¹H NMR (400 MHz, DMSO-*d*₆) δ ppm 4.36 (d, $J = 5.52$ Hz, 1 H), 6.11 (s, 1 H), 6.59 (t, $J = 7.36$ Hz, 1 H), 6.70 (d, $J = 7.67$ Hz, 2 H), 7.06–7.14 (m, 2 H), 7.70 (dd, $J = 8.75, 2.30$ Hz, 1 H), 8.21 (d, $J = 9.21$ Hz, 1 H), 8.24 (d, $J = 2.15$ Hz, 1 H), 12.79 (s, 1 H).

8-Chloro-2-[(2-hydroxyphenyl)amino]methyl[1]benzothieno[3,2-*d*]pyrimidin-4(3*H*)-one (6m): LCMS (APCI) m/z 358 ($M + H$)⁺; ¹H NMR (500 MHz, DMSO-*d*₆) δ ppm 4.38 (s, 2 H), 5.57 (s, 1 H), 6.40–6.50 (m, 1 H), 6.53–6.65 (m, 2 H), 6.70 (dd, $J = 7.63, 1.22$ Hz, 1 H), 7.71 (dd, $J = 8.70, 2.29$ Hz, 1 H), 8.18 (d, $J = 2.14$ Hz, 1 H), 8.22 (d, $J = 8.54$ Hz, 1 H), 9.43 (s, 1 H), 12.82 (s, 1 H).

8-Chloro-2-[(3-hydroxyphenyl)amino]methyl[1]benzothieno[3,2-*d*]pyrimidin-4(3*H*)-one (6n): LCMS (APCI) m/z 358 ($M + H$)⁺; ¹H NMR (500 MHz, DMSO-*d*₆) δ ppm 4.31 (d, $J = 5.80$ Hz, 2 H), 5.99–6.05 (m, 2 H), 6.11 (t, $J = 2.14$ Hz, 1 H), 6.15 (dd, $J = 7.93, 1.53$ Hz, 1 H), 6.87 (t, $J = 7.93$ Hz, 1 H), 7.71 (dd, $J = 8.54, 2.14$ Hz, 1 H), 8.22 (d, $J = 8.85$ Hz, 1 H), 8.26 (d, $J = 2.14$ Hz, 1 H), 9.01 (s, 1 H), 12.76 (s, 1 H).

8-Chloro-2-[(4-hydroxyphenyl)amino]methyl[1]benzothieno[3,2-*d*]pyrimidin-4(3*H*)-one (6o): LCMS (APCI) m/z 358 ($M + H$)⁺; ¹H NMR (500 MHz, DMSO-*d*₆) δ ppm 4.31 (s, 2 H), 6.56–6.61 (m, 2 H), 6.61–6.69 (m, 2 H), 7.72 (dd, $J = 8.54, 2.14$ Hz, 1 H), 8.22 (d, $J = 8.54$ Hz, 1 H), 8.27 (d, $J = 2.14$ Hz, 1 H), 8.64 (br s, 1 H), 12.75 (br s, 1 H).

8-Chloro-2-[(3-methoxyphenylamino)methyl][1]benzothieno[3,2-*d*]pyrimidin-4(3*H*)-one (6p): LCMS (APCI) m/z 372 ($M + H$)⁺; ¹H NMR (500 MHz, DMSO-*d*₆) δ ppm 3.66 (s, 1 H), 4.34 (d, $J = 6.10$ Hz, 2 H), 6.13–6.20 (m, 2 H), 6.28–6.31 (m, 2 H), 7.00 (t, $J = 8.24$ Hz, 1 H), 7.71 (dd, $J = 8.54, 2.14$ Hz, 1 H), 8.22 (d, $J = 8.54$ Hz, 1 H), 8.25 (d, $J = 2.14$ Hz, 1 H), 12.82 (s, 1 H).

8-Chloro-2-[(3,5-dihydroxyphenyl)amino]methyl[1]benzothieno[3,2-*d*]pyrimidin-4(3*H*)-one (6q): LCMS (APCI) m/z 374 ($M + H$)⁺; ¹H NMR (500 MHz, DMSO-*d*₆) δ ppm 4.25 (d, $J = 3.66$ Hz,

2 H), 5.53 (t, $J = 1.98$ Hz, 1 H), 5.60 (d, $J = 1.83$ Hz, 2 H), 5.88 (s, 1 H), 7.72 (dd, $J = 8.70, 2.29$ Hz, 1 H), 8.22 (d, $J = 8.85$ Hz, 1 H), 8.26 (d, $J = 2.14$ Hz, 1 H), 8.82 (s, 2 H), 12.70 (s, 1 H).

8-Chloro-2-[(3-hydroxy-2-methylphenyl)amino]methyl[1]benzothieno[3,2-*d*]pyrimidin-4(3*H*)-one (6r): LCMS (APCI) m/z 372 ($M + H$)⁺; ¹H NMR (500 MHz, DMSO-*d*₆) δ ppm 2.04 (s, 3 H), 4.39 (d, $J = 5.19$ Hz, 2 H), 5.47 (s, 1 H), 6.05 (d, $J = 7.93$ Hz, 1 H), 6.18 (d, $J = 7.93$ Hz, 1 H), 6.73 (t, $J = 8.09$ Hz, 1 H), 7.72 (dd, $J = 8.85, 2.14$ Hz, 1 H), 8.20 (d, $J = 2.14$ Hz, 1 H), 8.22 (d, $J = 8.85$ Hz, 1 H), 8.96 (s, 1 H), 12.71 (s, 1 H).

8-Chloro-2-[(3-hydroxy-4-methylphenyl)amino]methyl[1]benzothieno[3,2-*d*]pyrimidin-4(3*H*)-one (6s): LCMS (APCI) m/z 372 ($M + H$)⁺; ¹H NMR (500 MHz, DMSO-*d*₆) δ ppm 1.94 (s, 3 H), 4.28 (s, 2 H), 5.82 (br s, 1 H), 6.07 (dd, $J = 8.09, 2.29$ Hz, 1 H), 6.17 (d, $J = 2.14$ Hz, 1 H), 6.75 (d, $J = 7.93$ Hz, 2 H), 7.71 (dd, $J = 8.54, 2.14$ Hz, 1 H), 8.22 (d, $J = 8.54$ Hz, 1 H), 8.26 (d, $J = 1.83$ Hz, 1 H), 8.89 (s, 1 H), 12.70 (s, 1 H).

8-Chloro-2-[(2-(3-hydroxyphenyl)ethyl)amino]methyl[1]benzothieno[3,2-*d*]pyrimidin-4(3*H*)-one (6t): LCMS (APCI) m/z 386 ($M + H$)⁺; ¹H NMR (400 MHz, DMSO-*d*₆) δ ppm 1.26 (t, $J = 6.87$ Hz, 2 H), 2.95–2.98 (m, 2 H), 4.37 (s, 2 H), 6.53 (br s, 1 H), 6.65–6.70 (m, 2 H), 6.72 (d, $J = 7.93$ Hz, 1 H), 7.15 (t, $J = 8.09$ Hz, 1 H), 7.77 (dd, $J = 8.85, 2.14$ Hz, 1 H), 8.28 (d, $J = 8.85$ Hz, 1 H), 8.32 (d, $J = 2.14$ Hz, 1 H), 9.27 (s, 1 H), 9.42 (s, 1 H).

8-Chloro-2-[(3-hydroxyphenoxy)methyl][1]benzothieno[3,2-*d*]pyrimidin-4(3*H*)-one (7): A mixture of **4** (30 mg, 0.076 mmol), K₂CO₃ (52 mg, 0.38 mmol), and resorcinol (84 mg, 0.76 mmol) in DMF (2 mL) was stirred at 50 °C for 20 h and concentrated. The residue was purified by reverse-phase preparative HPLC to provide the title compound in 56% yield: ¹H NMR (400 MHz, DMSO-*d*₆) δ ppm 5.07 (s, 2 H), 6.41 (dd, $J = 7.98, 2.15$ Hz, 1 H), 6.48 (t, $J = 2.30$ Hz, 1 H), 6.49–6.54 (m, 1 H), 7.09 (t, $J = 8.13$ Hz, 1 H), 7.72 (dd, $J = 8.75, 1.99$ Hz, 1 H), 8.19 (d, $J = 2.15$ Hz, 1 H), 8.24 (d, $J = 8.59$ Hz, 1 H), 9.46 (s, 1 H), 13.11 (s, 1 H).

2-[(Dimethylamino)methyl]-8-bromo[1]benzothieno[3,2-*d*]pyrimidin-4(3*H*)-one (8): The title compound was prepared using the same synthetic sequences described for **6a**: LCMS (APCI) m/z 338 ($M + H$)⁺; ¹H NMR (500 MHz, methanol-*d*₄) δ ppm 3.17 (s, 6 H), 4.56 (s, 2 H), 7.79 (dd, $J = 8.70, 1.98$ Hz, 1 H), 8.00 (d, $J = 8.54$ Hz, 1 H), 8.56 (d, $J = 1.83$ Hz, 1 H).

2-[(Dimethylamino)methyl]-8-bromo[1]benzothieno[3,2-*d*]pyrimidin-4(3*H*)-one (9): The title compound was prepared using the same synthetic sequences described for **6a**: LCMS (APCI) m/z 260 ($M + H$)⁺; ¹H NMR (400 MHz, DMSO-*d*₆) δ ppm 3.03 (s, 6 H), 4.50 (s, 2 H), 7.66 (t, $J = 7.02$ Hz, 1 H), 7.69–7.75 (m, 1 H), 8.21 (d, $J = 7.93$ Hz, 1 H), 8.35 (d, $J = 7.32$ Hz, 1 H), 10.05 (s, 1 H), 13.17 (s, 1 H).

2-[(Dimethylamino)methyl]-8-methyl[1]benzothieno[3,2-*d*]pyrimidin-4(3*H*)-one (10a): The title compound was prepared using the same synthetic sequences described for **6a**: LCMS (APCI) m/z 274 ($M + H$)⁺; ¹H NMR (500 MHz, DMSO-*d*₆) δ ppm 2.52 (s, 3 H), 3.04 (s, 6 H), 4.50 (s, 2 H), 7.54 (dd, $J = 8.54, 1.53$ Hz, 1 H), 8.07 (d, $J = 8.24$ Hz, 1 H), 8.15 (s, 1 H), 10.19 (s, 1 H), 13.16 (s, 1 H).

2-[(Dimethylamino)methyl]-8-(trifluoromethyl)[1]benzothieno[3,2-*d*]pyrimidin-4(3*H*)-one (10b): The title compound was prepared using the same synthetic sequences described for **6a**: LCMS (APCI) m/z 328 ($M + H$)⁺; ¹H NMR (400 MHz, DMSO-*d*₆) δ ppm 2.99 (s, 6 H), 4.45 (s, 2 H), 8.03 (dd, $J = 8.59, 1.84$ Hz, 1 H), 8.49 (d, $J = 8.29$ Hz, 1 H), 8.63 (s, 1 H).

2-[(Dimethylamino)methyl]-8-ethyl[1]benzothieno[3,2-*d*]pyrimidin-4(3*H*)-one (11a): A mixture of **12a** (20 mg, 0.07 mmol) and 10% Pd/C (20 mg) in methanol (8 mL) was stirred under hydrogen atmosphere at room temperature overnight. The insoluble material was filtered off through Celite, and the filtrate was concentrated to give the desired product in quantitative yield: LCMS (APCI) m/z 288 ($M + H$)⁺; ¹H NMR (400 MHz, DMSO-*d*₆) δ ppm 1.29 (t, $J = 7.52$ Hz, 3 H), 2.83 (q, $J = 7.67$ Hz, 2 H), 3.01 (s, 6 H), 4.46 (s, 2 H), 7.58 (dd, $J = 8.29, 1.84$ Hz, 1 H), 8.09 (d, $J = 8.29$ Hz, 1 H), 8.16 (d, $J = 1.23$ Hz, 1 H).

2-[(Dimethylamino)methyl]-8-isopropyl[1]benzothieno[3,2-*d*]pyrimidin-4(3*H*)-one (11b). The title compound was prepared using the same synthetic sequences described for **6a**: LCMS (APCI) m/z 302 ($M + H$)⁺; ¹H NMR (400 MHz, DMSO-*d*₆) δ ppm 0.94 (t, $J = 7.32$ Hz, 3 H), 1.65–1.74 (m, 2 H), 2.71–2.81 (m, 2 H), 3.03 (s, 6 H), 4.49 (s, 2 H), 7.57 (dd, $J = 8.39, 1.68$ Hz, 1 H), 8.10 (d, $J = 8.24$ Hz, 1 H), 8.14 (s, 1 H), 9.93 (s, 1 H), 13.14 (s, 1 H).

2-[(Dimethylamino)methyl]-8-vinyl[1]benzothieno[3,2-*d*]pyrimidin-4(3*H*)-one (12a). The title compound was prepared using a procedure similar to that described for the synthesis of **14j**: LCMS (APCI) m/z 285 ($M + H$)⁺; ¹H NMR (400 MHz, DMSO-*d*₆) δ ppm 3.04 (s, 6 H), 4.49 (s, 2 H), 5.43 (d, $J = 11.35$ Hz, 1 H), 6.00 (d, $J = 17.49$ Hz, 1 H), 6.96 (dd, $J = 17.49, 11.05$ Hz, 1 H), 7.89 (dd, $J = 8.59, 1.84$ Hz, 1 H), 8.17 (d, $J = 8.59$ Hz, 1 H), 8.32 (s, 1 H), 10.01 (s, 1 H), 13.17 (s, 1 H).

8-[(*E*)-2-Cyclopropylvinyl]-2-[(dimethylamino)methyl][1]benzothieno[3,2-*d*]pyrimidin-4(3*H*)-one (12b). The title compound was prepared using a procedure similar to that described for the synthesis of **14j**: LCMS (APCI) m/z 326 ($M + H$)⁺; ¹H NMR (400 MHz, DMSO-*d*₆) δ ppm 0.55–0.59 (m, 2 H), 0.82–0.87 (m, 2 H), 1.61–1.71 (m, 1 H), 3.04 (s, 6 H), 4.49 (s, 2 H), 6.02 (dd, $J = 15.80, 9.05$ Hz, 1 H), 6.67 (d, $J = 15.96$ Hz, 1 H), 7.75 (dd, $J = 8.59, 1.84$ Hz, 1 H), 8.09 (d, $J = 8.29$ Hz, 1 H), 8.19 (d, $J = 1.53$ Hz, 1 H), 10.09 (s, 1 H), 13.16 (s, 1 H).

2-[(Dimethylamino)methyl]-8-ethynyl[1]benzothieno[3,2-*d*]pyrimidin-4(3*H*)-one (13a). To a mixture of **8** (60 mg, 0.18 mmol), ethynyltrimethylsilane (0.073 mL, 0.53 mmol), tetrakis(triphenylphosphine)palladium(0) (30.7 mg, 0.03 mmol), and triethylamine (0.074 mL, 0.53 mmol) in *N,N*-dimethylformamide (3 mL) was added copper(I) iodide (6.8 mg, 0.036 mmol), and the mixture was heated at 100 °C for 600 s in a CEM microwave synthesizer. After concentration, the residue was purified by reverse-phase preparative HPLC to provide the TMS-protected **13a** in 81% yield. This TMS-protected product (20 mg, 0.06 mmol) in methanol (1 mL) was treated with 5 M aqueous NaOH (1 mL) for 10 min and concentrated. The residue was purified by reverse-phase preparative HPLC to give the title compound as the TFA salt in 91% yield: LCMS (APCI) m/z 284 ($M + H$)⁺; ¹H NMR (400 MHz, DMSO-*d*₆) δ ppm 3.03 (s, 6 H), 4.36 (s, 1 H), 4.50 (s, 2 H), 7.76 (dd, $J = 8.44, 1.69$ Hz, 1 H), 8.24 (d, $J = 7.67$ Hz, 1 H), 8.46 (d, $J = 1.23$ Hz, 1 H), 9.82 (br s, 1 H), 13.24 (br s, 1 H).

2-[(Dimethylamino)methyl]-8-[3-(dimethylamino)prop-1-ynyl][1]benzothieno[3,2-*d*]pyrimidin-4(3*H*)-one (13b). The title compound was prepared using the same synthetic sequences as described for **13a**: LCMS (APCI) m/z 341 ($M + H$)⁺; ¹H NMR (400 MHz, DMSO-*d*₆) δ ppm 2.91 (s, 6 H), 3.00 (s, 6 H), 4.38 (s, 2 H), 4.46 (s, 2 H), 7.82 (dd, $J = 8.44, 1.69$ Hz, 1 H), 8.29 (d, $J = 8.59$ Hz, 1 H), 8.46 (d, $J = 1.53$ Hz, 1 H).

8-(6-Chlorohex-1-ynyl)-2-[(dimethylamino)methyl][1]benzothieno[3,2-*d*]pyrimidin-4(3*H*)-one. To a mixture of **8** (60 mg, 0.18 mmol), 6-chlorohex-1-yne (0.064 mL, 0.53 mmol), Pd(PPh₃)₄ (30.7 mg, 0.03 mmol), and triethylamine (0.074 mL, 0.53 mmol) in DMF (3 mL) was added CuI (6.8 mg, 0.036 mmol). The resulting mixture was heated at 100 °C for 600 s in a CEM microwave synthesizer and concentrated. The residue was purified by reverse-phase preparative HPLC to give the desired product as the TFA salt in 65% yield: LCMS (APCI) m/z 374 ($M + H$)⁺; ¹H NMR (400 MHz, DMSO-*d*₆) δ ppm 1.62–1.79 (m, 2 H), 1.83–1.98 (m, 2 H), 2.54 (t, $J = 7.21$ Hz, 2 H), 3.03 (s, 6 H), 3.72 (t, $J = 6.44$ Hz, 2 H), 4.50 (s, 2 H), 7.67 (dd, $J = 8.44, 1.69$ Hz, 1 H), 8.18 (d, $J = 8.29$ Hz, 1 H), 8.37 (d, $J = 1.23$ Hz, 1 H), 9.82 (s, 1 H), 13.20 (s, 1 H).

8-(6-(Piperidin-1-yl)hex-1-ynyl)-2-[(dimethylamino)methyl][1]benzothieno[3,2-*d*]pyrimidin-4(3*H*)-one (13c). 8-(6-Chlorohex-1-ynyl)-2-[(dimethylamino)methyl][1]benzothieno[3,2-*d*]pyrimidin-4(3*H*)-one (10 mg, 0.021 mmol) in piperidine (1.5 mL) was heated at 80 °C for 1 h. The reaction mixture was concentrated, and the residue was purified by HPLC to give the desired product as the TFA salt in 85% yield: LCMS (APCI) m/z 423 ($M + H$)⁺; ¹H

NMR (500 MHz, DMSO-*d*₆) δ ppm 1.32–1.49 (m, 1 H), 1.55–1.74 (m, 5 H), 1.75–1.89 (m, 4 H), 2.55 (t, $J = 7.17$ Hz, 2 H), 2.82–2.94 (m, 2 H), 3.03 (s, 6 H), 3.06–3.13 (m, 2 H), 3.40–3.62 (m, 2 H), 4.50 (s, 2 H), 7.67 (dd, $J = 8.54, 1.83$ Hz, 1 H), 8.20 (d, $J = 8.54$ Hz, 1 H), 8.36 (d, $J = 1.22$ Hz, 1 H), 9.29 (s, 1 H), 10.11 (br s, 1 H), 13.24 (br s, 1 H).

Compounds **14a–14q**, **15a–15d**, and **16a–16b** were prepared under Suzuki coupling conditions as described for the synthesis of **14j**.

2-[(Dimethylamino)methyl]-8-phenyl[1]benzothieno[3,2-*d*]pyrimidin-4(3*H*)-one (14a): LCMS (APCI) m/z 336 ($M + H$)⁺; ¹H NMR (400 MHz, DMSO-*d*₆) δ ppm 3.05 (s, 6 H), 4.51 (s, 2 H), 7.45 (t, $J = 7.36$ Hz, 1 H), 7.56 (t, $J = 7.67$ Hz, 2 H), 7.74–7.83 (m, 2 H), 8.02 (dd, $J = 8.59, 1.84$ Hz, 1 H), 8.30 (d, $J = 8.90$ Hz, 1 H), 8.57 (d, $J = 1.53$ Hz, 1 H), 9.89 (s, 1 H), 13.20 (s, 1 H).

2-[(Dimethylamino)methyl]-8-(1-phenylethyl)[1]benzothieno[3,2-*d*]pyrimidin-4(3*H*)-one (14b): LCMS (APCI) m/z 364 ($M + H$)⁺; ¹H NMR (500 MHz, DMSO-*d*₆) δ ppm 1.70 (d, $J = 7.02$ Hz, 3 H), 3.02 (s, 6 H), 4.41 (q, $J = 7.02$ Hz, 1 H), 4.48 (s, 2 H), 7.15–7.23 (m, 1 H), 7.24–7.34 (m, 4 H), 7.60 (dd, $J = 8.54, 1.83$ Hz, 1 H), 8.10 (d, $J = 8.54$ Hz, 1 H), 8.23 (d, $J = 1.53$ Hz, 1 H), 10.04 (br s, 1 H), 13.15 (br s, 1 H).

2-[(Dimethylamino)methyl]-8-(3-fluorophenyl)[1]benzothieno[3,2-*d*]pyrimidin-4(3*H*)-one (14c): LCMS (APCI) m/z 354 ($M + H$)⁺; ¹H NMR (400 MHz, DMSO-*d*₆) δ ppm 3.05 (s, 6 H), 4.51 (s, 2 H), 7.25–7.32 (m, 1 H), 7.57–7.66 (m, 3 H), 8.05 (dd, $J = 8.44, 1.99$ Hz, 1 H), 8.31 (d, $J = 9.21$ Hz, 1 H), 8.58 (d, $J = 1.23$ Hz, 1 H), 9.88 (s, 1 H), 13.22 (s, 1 H).

8-(3-Chlorophenyl)-2-[(dimethylamino)methyl][1]benzothieno[3,2-*d*]pyrimidin-4(3*H*)-one (14d): LCMS (APCI) m/z 370 ($M + H$)⁺; ¹H NMR (500 MHz, DMSO-*d*₆) δ ppm 3.03 (s, 6 H), 4.50 (s, 2 H), 7.50–7.55 (m, 1 H), 7.59 (t, $J = 7.93$ Hz, 1 H), 7.76 (d, $J = 7.93$ Hz, 1 H), 7.84 (t, $J = 1.83$ Hz, 1 H), 8.05 (dd, $J = 8.54, 1.83$ Hz, 1 H), 8.32 (d, $J = 8.24$ Hz, 1 H), 8.56 (d, $J = 1.53$ Hz, 1 H), 9.88 (br s, 1 H), 13.23 (br s, 1 H).

2-[(Dimethylamino)methyl]-8-[3-(trifluoromethoxy)phenyl][1]benzothieno[3,2-*d*]pyrimidin-4(3*H*)-one (14e): LCMS (APCI) m/z 420 ($M + H$)⁺; ¹H NMR (400 MHz, DMSO-*d*₆) δ ppm 3.05 (s, 6 H), 4.51 (s, 2 H), 7.44–7.49 (m, 1 H), 7.70 (t, $J = 7.98$ Hz, 1 H), 7.75 (s, 1 H), 7.84 (d, $J = 8.59$ Hz, 1 H), 8.06 (dd, $J = 8.44, 1.99$ Hz, 1 H), 8.33 (d, $J = 8.59$ Hz, 1 H), 8.57 (d, $J = 1.23$ Hz, 1 H), 10.01 (s, 1 H), 13.21 (s, 1 H).

2-[(Dimethylamino)methyl]-8-(3-hydroxyphenyl)[1]benzothieno[3,2-*d*]pyrimidin-4(3*H*)-one (14f): LCMS (APCI) m/z 352 ($M + H$)⁺; ¹H NMR (500 MHz, DMSO-*d*₆) δ ppm 3.01 (s, 6 H), 4.50 (s, 2 H), 6.85 (dd, $J = 7.93, 1.53$ Hz, 1 H), 7.13 (t, $J = 1.98$ Hz, 1 H), 7.19 (d, $J = 7.63$ Hz, 1 H), 7.34 (t, $J = 7.93$ Hz, 1 H), 7.94 (dd, $J = 8.54, 1.83$ Hz, 1 H), 8.27 (d, $J = 8.54$ Hz, 1 H), 8.52 (d, $J = 1.53$ Hz, 1 H), 9.66 (br s, 1 H), 9.85 (br s, 1 H), 13.20 (br s, 1 H).

2-[(Dimethylamino)methyl]-8-(2-methylphenyl)[1]benzothieno[3,2-*d*]pyrimidin-4(3*H*)-one (14g): LCMS (APCI) m/z 350 ($M + H$)⁺; ¹H NMR (400 MHz, DMSO-*d*₆) δ ppm 2.26 (s, 3 H), 2.98 (s, 6 H), 4.46 (s, 1 H), 7.26–7.40 (m, 4 H), 7.69 (dd, $J = 8.29, 2.15$ Hz, 1 H), 8.25 (d, $J = 8.29$ Hz, 1 H), 8.26 (s, 1 H).

2-[(Dimethylamino)methyl]-8-(4-ethylphenyl)[1]benzothieno[3,2-*d*]pyrimidin-4(3*H*)-one (14h): LCMS (APCI) m/z 363 ($M + H$)⁺; ¹H NMR (500 MHz, DMSO-*d*₆) δ ppm 1.24 (t, $J = 7.63$ Hz, 3 H), 2.69 (q, $J = 7.63$ Hz, 2 H), 3.04 (s, 6 H), 4.51 (s, 2 H), 7.39 (d, $J = 8.24$ Hz, 2 H), 7.70 (d, $J = 8.24$ Hz, 2 H), 8.00 (dd, $J = 8.54, 2.14$ Hz, 1 H), 8.28 (d, $J = 8.54$ Hz, 1 H), 8.55 (d, $J = 1.83$ Hz, 1 H), 9.90 (br s, 1 H), 13.18 (br s, 1 H).

4-[2-[(Dimethylamino)methyl]-4-oxo-3,4-dihydro[1]benzothieno[3,2-*d*]pyrimidin-8-yl]benzonitrile (14i): LCMS (APCI) m/z 361 ($M + H$)⁺; ¹H NMR (400 MHz, DMSO-*d*₆) δ ppm 3.01 (s, 6 H), 4.47 (s, 2 H), 7.97–8.05 (m, 4 H), 8.09 (dd, $J = 8.59, 1.84$ Hz, 1 H), 8.36 (d, $J = 8.59$ Hz, 1 H), 8.61 (d, $J = 1.23$ Hz, 1 H).

8-(4-Hydroxyphenyl)-2-[(dimethylamino)methyl][1]benzothieno[3,2-*d*]pyrimidin-4(3*H*)-one (14j). To a mixture of **8** (40 mg, 0.11 mmol), Pd(PPh₃)₂Cl₂ (8.3 g, 0.012 mmol), and 4-hydroxyphenyl boronic acid (19.9 mg, 0.14 mmol) in 2.5 mL of DME/EtOH/H₂O

(7:2:3) was added 1 M Na₂CO₃ aqueous solution (0.2 mL). The reaction mixture was heated for 600 s in a CEM microwave synthesizer at 150 °C and concentrated. The residue was purified by HPLC to give the desired product as the TFA salt (33 mg, 65%). The TFA salt was converted into the HCl salt as follows: To a solution of the TFA salt product in methanol was added a large excess of 1 M HCl in ether. The resulting mixture was stirred at room temperature for 4 h, and the white precipitate was collected by filtration and dried at 60 °C for 3 days to give the title compound as the HCl salt: LCMS (APCI) *m/z* 352 (M + H)⁺; ¹H NMR (500 MHz, DMSO-*d*₆) δ ppm 3.02 (s, 6 H), 4.52 (s, 2 H), 6.94 (d, *J* = 8.54 Hz, 2 H), 7.63 (d, *J* = 8.54 Hz, 2 H), 7.93 (dd, *J* = 8.54, 1.83 Hz, 1 H), 8.21 (d, *J* = 8.54 Hz, 1 H), 8.52 (d, *J* = 1.53 Hz, 1 H), 9.73 (s, 1 H), 10.36 (br s, 1 H), 13.23 (br s, 1 H). Anal. (C₁₉H₁₇N₃O₂S·HCl·0.35H₂O) C, H, N, Cl. HRMS (ESI-TOF) calcd for C₁₉H₁₈N₃O₂S (M + H)⁺ 352.1120; found 352.1122.

8-(4-Aminophenyl)-2-[(dimethylamino)methyl][1]benzothieno[3,2-*d*]pyrimidin-4(3*H*)-one (14k): LCMS (APCI) *m/z* 351 (M + H)⁺; ¹H NMR (400 MHz, DMSO-*d*₆) δ ppm 3.04 (s, 6 H), 4.51 (s, 2 H), 6.86 (d, *J* = 8.59 Hz, 2 H), 7.57 (d, *J* = 8.59 Hz, 2 H), 7.92 (dd, *J* = 8.59, 2.15 Hz, 1 H), 8.19 (d, *J* = 8.59 Hz, 1 H), 8.47 (d, *J* = 1.53 Hz, 1 H), 13.17 (s, 1 H).

2-[(Dimethylamino)methyl]-8-[4-(trifluoromethoxy)phenyl][1]benzothieno[3,2-*d*]pyrimidin-4(3*H*)-one (14l): LCMS (APCI) *m/z* 420 (M + H)⁺; ¹H NMR (400 MHz, DMSO-*d*₆) δ ppm 3.04 (s, 6 H), 4.50 (s, 2 H), 7.56 (d, *J* = 8.59 Hz, 2 H), 7.90 (d, *J* = 8.59 Hz, 2 H), 8.03 (dd, *J* = 8.44, 1.69 Hz, 1 H), 8.32 (d, *J* = 8.59 Hz, 1 H), 8.56 (d, *J* = 1.84 Hz, 1 H), 13.20 (s, 1 H).

2-[(Dimethylamino)methyl]-8-(3-fluoro-4-hydroxyphenyl)[1]benzothieno[3,2-*d*]pyrimidin-4(3*H*)-one (14m): LCMS (APCI) *m/z* 370 (M + H)⁺; ¹H NMR (500 MHz, DMSO-*d*₆) δ ppm 3.05 (s, 6 H), 4.51 (s, 2 H), 7.12 (t, *J* = 8.70 Hz, 1 H), 7.45 (dd, *J* = 8.09, 1.98 Hz, 1 H), 7.59 (dd, *J* = 12.66, 2.29 Hz, 1 H), 7.94–8.00 (m, 1 H), 8.25 (d, *J* = 8.54 Hz, 1 H), 8.49 (d, *J* = 1.53 Hz, 1 H), 9.86 (s, 1 H), 10.14 (s, 1 H), 13.20 (s, 1 H).

2-[(Dimethylamino)methyl]-8-[4-dimethylaminophenyl][1]benzothieno[3,2-*d*]pyrimidin-4(3*H*)-one (14n): LCMS (APCI) *m/z* 379 (M + H)⁺; ¹H NMR (500 MHz, DMSO-*d*₆) δ ppm 2.98 (s, 6 H), 3.05 (s, 6 H), 4.52 (s, 2 H), 6.89 (d, *J* = 8.85 Hz, 2 H), 7.65 (d, *J* = 8.85 Hz, 2 H), 7.96 (dd, *J* = 8.54, 2.14 Hz, 1 H), 8.20 (d, *J* = 8.54 Hz, 1 H), 8.49 (d, *J* = 1.83 Hz, 1 H), 9.94 (s, 1 H), 13.18 (s, 1 H).

8-(4-Chloro-3-fluorophenyl)-2-[(dimethylamino)methyl][1]benzothieno[3,2-*d*]pyrimidin-4(3*H*)-one (14o): LCMS (APCI) *m/z* 388 (M + H)⁺; ¹H NMR (500 MHz, DMSO-*d*₆) δ ppm 3.03 (s, 6 H), 4.49 (s, 2 H), 7.65–7.70 (m, 1 H), 7.73–7.81 (m, 1 H), 7.87 (dd, *J* = 10.74, 2.15 Hz, 1 H), 8.06 (dd, *J* = 8.59, 2.15 Hz, 1 H), 8.32 (d, *J* = 9.21 Hz, 1 H), 8.58 (d, *J* = 1.23 Hz, 1 H).

8-(3-Chloro-5-fluorophenyl)-2-[(dimethylamino)methyl][1]benzothieno[3,2-*d*]pyrimidin-4(3*H*)-one (14p): LCMS (APCI) *m/z* 388 (M + H)⁺; ¹H NMR (500 MHz, DMSO-*d*₆) δ ppm 3.03 (s, 6 H), 4.48 (s, 2 H), 7.48–7.58 (m, 1 H), 7.67 (d, *J* = 9.82 Hz, 1 H), 7.73 (s, 1 H), 8.08 (dd, *J* = 8.59, 1.53 Hz, 1 H), 8.33 (d, *J* = 8.59 Hz, 1 H), 8.57 (d, *J* = 1.53 Hz, 1 H).

8-(3,5-Dichlorophenyl)-2-[(dimethylamino)methyl][1]benzothieno[3,2-*d*]pyrimidin-4(3*H*)-one (14q): LCMS (APCI) *m/z* 404 (M + H)⁺; ¹H NMR (400 MHz, DMSO-*d*₆) δ ppm 3.02 (s, 6 H), 4.48 (s, 2 H), 7.70 (t, *J* = 1.84 Hz, 1 H), 7.84 (d, *J* = 1.84 Hz, 2 H), 8.08 (dd, *J* = 8.59, 1.84 Hz, 1 H), 8.33 (d, *J* = 8.59 Hz, 1 H), 8.56 (d, *J* = 1.53 Hz, 1 H).

2-[(Dimethylamino)methyl]-8-thien-3-yl[1]benzothieno[3,2-*d*]pyrimidin-4(3*H*)-one (15a): LCMS (APCI) *m/z* 342 (M + H)⁺; ¹H NMR (400 MHz, DMSO-*d*₆) δ ppm 3.05 (s, 6 H), 7.66 (dd, *J* = 5.06, 1.38 Hz, 1 H), 7.75 (dd, *J* = 5.06, 2.92 Hz, 1 H), 8.00 (dd, *J* = 2.92, 1.38 Hz, 1 H), 8.08 (dd, *J* = 8.44, 1.99 Hz, 1 H), 8.24 (d, *J* = 8.59 Hz, 1 H), 8.57 (d, *J* = 1.53 Hz, 1 H), 10.00 (s, 1 H), 13.16 (s, 1 H).

2-[(Dimethylamino)methyl]-8-(1*H*-pyrrol-2-yl)[1]benzothieno[3,2-*d*]pyrimidin-4(3*H*)-one (15b): LCMS (APCI) *m/z* 325 (M + H)⁺; ¹H NMR (500 MHz, DMSO-*d*₆) δ ppm 3.06 (s, 6 H), 4.47 (s, 2 H), 6.08–6.27 (m, 1 H), 6.56–6.69 (m, 1 H), 6.86–7.01 (m,

1 H), 7.97 (dd, *J* = 8.54, 1.83 Hz, 1 H), 8.16 (d, *J* = 8.54 Hz, 1 H), 8.49 (d, *J* = 1.53 Hz, 1 H), 10.05 (br s, 1 H), 11.54 (s, 1 H), 13.14 (br s, 1 H).

2-[(Dimethylamino)methyl]-8-(3-furyl)[1]benzothieno[3,2-*d*]pyrimidin-4(3*H*)-one (15c): LCMS (APCI) *m/z* 326 (M + H)⁺; ¹H NMR (500 MHz, DMSO-*d*₆) δ ppm 3.06 (s, 6 H), 4.51 (s, 2 H), 7.06 (s, 1 H), 7.84 (t, *J* = 1.53 Hz, 1 H), 7.97 (dd, *J* = 8.90, 1.84 Hz, 1 H), 8.21 (d, *J* = 8.29 Hz, 1 H), 8.32 (s, 1 H), 8.45 (d, *J* = 1.84 Hz, 1 H), 10.27 (s, 1 H), 13.20 (s, 1 H).

2-[(Dimethylamino)methyl]-8-(4-methylthien-3-yl)[1]benzothieno[3,2-*d*]pyrimidin-4(3*H*)-one (15d): LCMS (APCI) *m/z* 356 (M + H)⁺; ¹H NMR (500 MHz, DMSO-*d*₆) δ ppm 2.28 (s, 3 H), 3.02 (s, 6 H), 4.50 (s, 2 H), 7.37 (d, *J* = 2.44 Hz, 1 H), 7.59 (d, *J* = 3.36 Hz, 1 H), 7.76 (dd, *J* = 8.24, 1.83 Hz, 1 H), 8.25 (d, *J* = 8.24 Hz, 1 H), 8.34 (d, *J* = 1.22 Hz, 1 H), 9.85 (s, 1 H), 13.20 (s, 1 H).

2-[(Dimethylamino)methyl]-8-pyridin-3-yl[1]benzothieno[3,2-*d*]pyrimidin-4(3*H*)-one (16a): LCMS (APCI) *m/z* 337 (M + H)⁺; ¹H NMR (500 MHz, DMSO-*d*₆) δ ppm 3.05 (s, 6 H), 4.52 (s, 2 H), 7.65 (dd, *J* = 7.93, 4.88 Hz, 1 H), 8.09 (dd, *J* = 8.54, 1.83 Hz, 1 H), 8.28 (d, *J* = 8.24 Hz, 1 H), 8.37 (d, *J* = 8.54 Hz, 1 H), 8.63 (d, *J* = 1.53 Hz, 1 H), 8.70 (dd, *J* = 4.88, 1.22 Hz, 1 H), 9.07 (d, *J* = 1.83 Hz, 1 H), 9.95 (br s, 1 H), 13.25 (br s, 1 H).

2-[(Dimethylamino)methyl]-8-pyrimidin-5-yl[1]benzothieno[3,2-*d*]pyrimidin-4(3*H*)-one (16b): LCMS (APCI) *m/z* 338 (M + H)⁺; ¹H NMR (400 MHz, DMSO-*d*₆) δ ppm 3.01 (s, 6 H), 4.45 (s, 2 H), 8.15 (dd, *J* = 8.44, 1.99 Hz, 1 H), 8.40 (d, *J* = 8.59 Hz, 1 H), 8.66 (d, *J* = 1.53 Hz, 1 H), 9.27 (s, 3 H).

2-[(Dimethylamino)methyl]-8-pyrrolidin-1-yl[1]benzothieno[3,2-*d*]pyrimidin-4(3*H*)-one (17a): To a mixture of biphenyl-2-yl-di-*tert*-butylphosphine (5.3 mg, 0.018 mmol), Pd₂(dba)₃ (4.1 mg, 0.0044 mmol), and NaOt-Bu (26 mg, 0.27 mmol) in toluene (2.5 mL) were added **8** (30 mg, 0.089 mmol) and pyrrolidine (0.015 mL, 0.18 mmol). The reaction mixture was purged with nitrogen, heated at 120 °C for 20 min in a CEM microwave synthesizer, and concentrated. The residue was purified by reverse-phase preparative HPLC to give the desired product as the TFA salt (25.6 mg, 52%): LCMS (APCI) *m/z* 329 (M + H)⁺; ¹H NMR (500 MHz, DMSO-*d*₆) δ ppm 1.98–2.06 (m, 4 H), 3.02 (s, 6 H), 3.34 (t, *J* = 6.41 Hz, 4 H), 4.48 (s, 2 H), 7.06 (dd, *J* = 8.85, 2.44 Hz, 1 H), 7.32 (d, *J* = 2.44 Hz, 1 H), 7.91 (d, *J* = 8.85 Hz, 1 H), 10.05 (s, 1 H), 13.04 (s, 1 H).

2-[(Dimethylamino)methyl]-8-piperidin-1-yl[1]benzothieno[3,2-*d*]pyrimidin-4(3*H*)-one (17b): The title compound was prepared using the same procedure as described for **17a**: LCMS (APCI) *m/z* 343 (M + H)⁺; ¹H NMR (500 MHz, DMSO-*d*₆) δ ppm 1.50–1.64 (m, 2 H), 1.64–1.81 (m, 4 H), 3.03 (s, 6 H), 3.19–3.36 (m, 4 H), 4.49 (s, 2 H), 7.49 (dd, *J* = 9.15, 2.44 Hz, 1 H), 7.77 (s, 1 H), 7.99 (d, *J* = 9.15 Hz, 1 H), 10.02 (br s, 1 H), 13.11 (br s, 1 H).

3-(4-(4,4,5,5-Tetramethyl-1,3,2-dioxaborolan-2-yl)phenoxy)propane-1,2-diol (18c): 4-(4,4,5,5-Tetramethyl-1,3,2-dioxaborolan-2-yl)phenol (220 mg, 1 mmol) in DME (5 mL) was treated with 3-chloropropane-1,2-diol (166 mg, 1.5 mmol) and potassium carbonate (691 mg, 5 mmol) and heated at 80 °C for 19 h. Additional 3-chloropropane-1,2-diol (166 mg, 1.5 mmol) was added, and heating was continued for 24 h. The reaction mixture was cooled to room temperature, filtered through Celite, concentrated, and purified by column chromatography on silica gel eluting with a solvent gradient of 0 to 1% MeOH in CH₂Cl₂ to give 86 mg (29%) of the title compound: MS (DCI) *m/z* 312 (M + NH₄)⁺.

8-[4-(2,3-Dihydroxypropoxy)phenyl]-2-[(dimethylamino)methyl][1]benzothieno[3,2-*d*]pyrimidin-4(3*H*)-one (18a): A mixture of **8** (34 mg, 0.1 mmol), **18c** (44 mg, 0.15 mmol), bis(triphenylphosphine)palladium(II) dichloride (7 mg, 0.01 mmol), and sodium carbonate (2 M, 0.15 mL, 0.3 mmol) in a 7:2:3 mixture of DME/EtOH/H₂O (3 mL) was heated via microwave for 10 min at 150 °C, cooled to room temperature, filtered through a syringe filter, concentrated, and purified by column chromatography on silica gel eluting with 1:1 EtOAc/MeOH. The product was further purified by reverse-phase preparative HPLC: ¹H NMR

(300 MHz, DMSO-*d*₆) δ ppm 2.95 (s, 6 H), 3.48 (d, *J* = 5.43 Hz, 2 H), 3.83 (dq, *J* = 5.26, 5.03 Hz, 1 H), 3.94 (m, 1 H), 4.08 (dd, *J* = 9.83, 4.41 Hz, 1 H), 4.40 (s, 2 H), 4.69 (s, 1 H), 4.97 (s, 1 H), 7.11 (m, 2 H), 7.72 (m, 2 H), 7.97 (dd, *J* = 8.65, 1.86 Hz, 1 H), 8.24 (d, *J* = 8.48 Hz, 1 H), 8.50 (d, *J* = 1.70 Hz, 1 H).

2-[(3-(4,4,5,5-Tetramethyl-1,3,2-dioxaborolan-2-yl)phenoxy)propyl]isoindoline-1,3-dione (18d). 4-(4,4,5,5-Tetramethyl-1,3,2-dioxaborolan-2-yl)phenol (220 mg, 1 mmol) in DME (5 mL) was treated with 2-(3-bromopropyl)isoindoline-1,3-dione (402 mg, 1.5 mmol) and potassium carbonate (691 mg, 5 mmol) and heated at 80 °C for 19 h. Additional 2-(3-bromopropyl)isoindoline-1,3-dione (305 mg, 1.14 mmol) was added, and heating was continued for 9 h. The reaction mixture was cooled to room temperature, filtered through Celite, concentrated, and purified by column chromatography on silica gel eluting with a solvent gradient of 0 to 1% MeOH in CH₂Cl₂: MS (ESI) *m/z* 408 (M + H)⁺; ¹H NMR (500 MHz, DMSO-*d*₆) δ ppm 2.05 (m, 2 H), 2.97 (s, 6 H), 3.00 (m, 2 H), 4.14 (t, *J* = 6.10 Hz, 2 H), 4.43 (s, 2 H), 7.11 (m, 2 H), 7.75 (m, 2 H), 7.82 (s, 2 H), 7.98 (dd, *J* = 8.54, 1.83 Hz, 1 H), 8.25 (d, *J* = 8.54 Hz, 1 H), 8.50 (d, *J* = 1.22 Hz, 1 H), 13.15 (s, 1 H).

8-[4-(3-Aminopropoxy)phenyl]-2-[(dimethylamino)methyl][1]benzothieno[3,2-*d*]pyrimidin-4(3*H*)-one (18b). A mixture of **8** (34 mg, 0.1 mmol), **18d** (61 mg, 0.15 mmol), bis(triphenylphosphine)palladium(II) dichloride (7 mg, 0.01 mmol), and sodium carbonate (2 M, 0.15 mL, 0.3 mmol) in a 7:2:3 mixture of DME/EtOH/H₂O (3 mL) was heated via microwave for 10 min at 150 °C, cooled to room temperature, filtered through a syringe filter, concentrated, and purified by column chromatography on silica gel eluting with 0–50% MeOH in EtOAc. The product was further purified by reverse-phase preparative HPLC: MS (ESI) *m/z* 409 (M + H)⁺; ¹H NMR (500 MHz, DMSO-*d*₆) δ ppm 2.05 (m, 2 H), 2.79 (s, 6 H), 3.00 (m, 2 H), 4.14 (t, *J* = 6.10 Hz, 2 H), 4.43 (s, 2 H), 7.11 (m, 2 H), 7.75 (m, 2 H), 7.82 (s, 2 H), 7.98 (dd, *J* = 8.54, 1.83 Hz, 1 H), 8.25 (d, *J* = 8.54 Hz, 1 H), 8.50 (d, *J* = 1.22 Hz, 1 H), 13.14 (s, 1 H).

Methyl 3-amino-5-bromobenzo[*b*]thiophene-2-carboxylate. To a cold solution of 5-bromo-2-fluorobenzonitrile (13.5 g, 67.5 mmol) in DMF at 0 °C was added dropwise methyl 2-mercaptoacetate (6.45 mL, 70.88 mmol). The reaction mixture was stirred at 0 °C for 30 min, and then 5 M NaOH aqueous solution (20.25 mL) was added dropwise. After stirring at 0 °C for 3 h, the reaction mixture was quenched with ice–water. The resulting precipitate was collected by filtration and dried to give 18.5 g of white solid in 96% yield: LCMS (APCI) *m/z* 287 (M + H)⁺.

5-Bromo-3-[(2-chloroacetimidoyl)amino]benzo[*b*]thiophene-2-carboxylic acid methyl ester. A suspension of methyl 3-amino-5-bromobenzo[*b*]thiophene-2-carboxylate (7.2 g, 25.16 mmol) in 4 N hydrochloric acid in dioxane (70 mL) was treated with 2-chloroacetonitrile (3.18 mL, 50.32 mmol) at room temperature for 3 h. The white solid was collected by filtration and dried to give the desired product as the HCl salt quantitatively: LCMS (APCI) *m/z* 362 (M + H)⁺.

2-[(3-Hydroxyphenyl)amino]methyl]-8-thien-3-yl[1]benzothieno[3,2-*d*]pyrimidin-4(3*H*)-one (19a). A mixture of 5-bromo-3-[(2-chloroacetimidoyl)amino]benzo[*b*]thiophene-2-carboxylic acid methyl ester (30 mg, 0.076 mmol) and 3-aminophenol (41 mg, 0.38 mmol) in DMF (2 mL) was stirred at room temperature overnight and concentrated. The residue was purified by reverse-phase preparative HPLC to provide the desired product as the TFA salt in 56% yield: LCMS (APCI) *m/z* 404 (M + H)⁺; ¹H NMR (500 MHz, DMSO-*d*₆) δ ppm 4.31 (d, *J* = 5.80 Hz, 2 H), 6.00–6.05 (m, 2 H), 6.11 (t, *J* = 2.14 Hz, 1 H), 6.15 (dd, *J* = 7.93, 1.53 Hz, 1 H), 6.87 (t, *J* = 7.93 Hz, 1 H), 7.82 (dd, *J* = 8.70, 1.98 Hz, 1 H), 8.15 (d, *J* = 8.85 Hz, 1 H), 8.40 (d, *J* = 1.83 Hz, 1 H), 9.02 (s, 1 H), 12.76 (br s, 1 H).

2-[(3-Hydroxyphenyl)amino]methyl]-8-thien-3-yl[1]benzothieno[3,2-*d*]pyrimidin-4(3*H*)-one (19b). The title compound was prepared under similar Suzuki coupling conditions as those described for the synthesis of **14j**: LCMS (APCI) *m/z* 406 (M + H)⁺;

¹H NMR (500 MHz, DMSO-*d*₆) δ ppm 4.33 (d, *J* = 4.88 Hz, 2 H), 6.03 (dd, *J* = 7.48, 1.98 Hz, 2 H), 6.13 (t, *J* = 2.14 Hz, 1 H), 6.16 (d, *J* = 7.93 Hz, 1 H), 6.87 (t, *J* = 8.09 Hz, 1 H), 7.72 (d, *J* = 2.14 Hz, 2 H), 8.03–8.11 (m, 2 H), 8.19 (d, *J* = 8.24 Hz, 1 H), 8.53 (d, *J* = 1.53 Hz, 1 H), 9.02 (s, 1 H), 12.68 (s, 1 H).

2-[(3-Hydroxyphenyl)amino]methyl]-8-phenyl[1]benzothieno[3,2-*d*]pyrimidin-4(3*H*)-one (19c). The title compound was prepared under similar Suzuki coupling conditions as those described for the synthesis of **14j**: LCMS (APCI) *m/z* 400 (M + H)⁺; ¹H NMR (500 MHz, DMSO-*d*₆) δ ppm 4.33 (d, *J* = 6.10 Hz, 2 H), 5.99–6.08 (m, 2 H), 6.13 (t, *J* = 2.14 Hz, 1 H), 6.14–6.21 (m, 1 H), 6.86 (t, *J* = 7.93 Hz, 1 H), 7.44 (t, *J* = 7.32 Hz, 1 H), 7.54 (t, *J* = 7.63 Hz, 2 H), 7.81 (d, *J* = 7.32 Hz, 2 H), 7.99 (dd, *J* = 8.54, 1.83 Hz, 1 H), 8.25 (d, *J* = 8.54 Hz, 1 H), 8.48 (d, *J* = 1.83 Hz, 1 H), 9.00 (s, 1 H), 12.70 (s, 1 H).

8-Bromo-2-[(3*S*)-3-hydroxypyrrolidin-1-yl]methyl[1]benzothieno[3,2-*d*]pyrimidin-4(3*H*)-one. The title compound was prepared using a procedure similar to that described for **6a**: LCMS (APCI) *m/z* 380 (M + H)⁺; ¹H NMR (500 MHz, DMSO-*d*₆) δ ppm 1.56–1.66 (m, 1 H), 1.97–2.09 (m, 1 H), 2.51–2.61 (m, 2 H), 2.75–2.87 (m, 2 H), 3.67–3.78 (m, 2 H), 4.09–4.28 (m, 1 H), 7.81 (dd, *J* = 8.54, 2.14 Hz, 1 H), 8.15 (d, *J* = 8.85 Hz, 1 H), 8.31 (d, *J* = 2.14 Hz, 1 H).

2-[(3*S*)-3-Hydroxypyrrolidin-1-yl]methyl]-8-thien-3-yl[1]benzothieno[3,2-*d*]pyrimidin-4(3*H*)-one (20a). The title compound was prepared under similar Suzuki coupling conditions as those described for the synthesis of **14j**: LCMS (APCI) *m/z* 384 (M + H)⁺; ¹H NMR (500 MHz, DMSO-*d*₆) δ ppm 2.00 (br s, 1 H), 2.04–2.37 (m, 1 H), 2.62–3.11 (m, 2 H), 3.69–4.10 (m, *J* = 73.54 Hz, 2 H), 4.51 (br s, 1 H), 4.63 (d, *J* = 13.43 Hz, 2 H), 5.55 (br s, 1 H), 7.66–7.71 (m, 1 H), 7.75 (dd, *J* = 5.03, 2.90 Hz, 1 H), 8.03 (dd, *J* = 2.90, 1.37 Hz, 1 H), 8.08 (dd, *J* = 8.54, 1.83 Hz, 1 H), 8.24 (d, *J* = 8.54 Hz, 1 H), 8.56 (s, 1 H), 10.47 (br s, 1 H), 13.15 (br s, 1 H).

2-[(3*S*)-3-Hydroxypyrrolidin-1-yl]methyl]-8-phenyl[1]benzothieno[3,2-*d*]pyrimidin-4(3*H*)-one (20b). The title compound was prepared under similar Suzuki coupling conditions as those described for the synthesis of **14j**: LCMS (APCI) *m/z* 378 (M + H)⁺; ¹H NMR (500 MHz, pyridine-*d*₅) δ ppm 1.98–2.10 (m, 1 H), 2.16–2.28 (m, 1 H), 2.87–2.98 (m, 1 H), 3.13–3.22 (m, 2 H), 3.22–3.30 (m, 1 H), 4.08–4.35 (m, 2 H), 4.58–4.75 (m, 1 H), 7.41 (t, *J* = 7.32 Hz, 1 H), 7.51 (t, *J* = 7.63 Hz, 2 H), 7.77 (d, *J* = 7.32 Hz, 2 H), 7.90 (dd, *J* = 8.39, 1.98 Hz, 1 H), 8.07 (d, *J* = 8.24 Hz, 1 H), 8.79 (d, *J* = 1.53 Hz, 1 H).

8-(4-Hydroxyphenyl)-2-[(3*S*)-3-hydroxypyrrolidin-1-yl]methyl]-[1]benzothieno[3,2-*d*]pyrimidin-4(3*H*)-one (20c). The title compound was prepared under similar Suzuki coupling conditions as those described for the synthesis of **14j**: LCMS (APCI) *m/z* 394 (M + H)⁺; ¹H NMR (500 MHz, DMSO-*d*₆) δ ppm 1.97 (br s, 1 H), 2.08–2.34 (m, 1 H), 3.34 (br s, 2 H), 3.87 (br s, 2 H), 4.49 (s, 1 H), 4.60 (br s, 2 H), 5.52 (s, 1 H), 6.93 (d, *J* = 8.85 Hz, 2 H), 7.61 (d, *J* = 8.54 Hz, 2 H), 7.93 (dd, *J* = 8.54, 1.83 Hz, 1 H), 8.22 (d, *J* = 8.54 Hz, 1 H), 8.45 (s, 1 H), 9.68 (s, 1 H), 10.17–10.72 (br s, 1 H), 13.12 (s, 1 H).

4-2-[(3*S*)-3-Hydroxypyrrolidin-1-yl]methyl]-4-oxo-3,4-dihydro[1]benzothieno[3,2-*d*]pyrimidin-8-yl]benzonitrile (20d). The title compound was prepared under similar Suzuki coupling conditions as those described for the synthesis of **14j**: LCMS (APCI) *m/z* 403 (M + H)⁺; ¹H NMR (500 MHz, pyridine-*d*₅) δ ppm 2.00–2.09 (m, 1 H), 2.16–2.27 (m, 1 H), 2.83–2.92 (m, 1 H), 3.10–3.19 (m, 2 H), 3.20–3.27 (m, 1 H), 4.08–4.30 (m, 2 H), 4.56–4.79 (m, 1 H), 7.58 (s, 2 H), 7.88 (dd, *J* = 8.39, 1.98 Hz, 1 H), 8.13 (d, *J* = 8.24 Hz, 1 H), 8.78 (d, *J* = 1.22 Hz, 1 H).

8-[(*E*)-2-Cyclopropylvinyl]-2-[(3*S*)-3-hydroxypyrrolidin-1-yl]methyl[1]benzothieno[3,2-*d*]pyrimidin-4(3*H*)-one (20e). The title compound was prepared under similar Suzuki coupling conditions as those described for the synthesis of **14j**: LCMS (APCI) *m/z* 368 (M + H)⁺; ¹H NMR (400 MHz, DMSO-*d*₆) δ ppm 0.53–0.62 (m, 2 H), 0.78–0.89 (m, 2 H), 1.56–1.74 (m, 1 H), 1.91–2.36 (m, 2 H), 3.76–4.04 (m, 2 H), 4.57 (d, *J* = 46.95 Hz,

3 H), 5.40 (s, 1 H), 6.03 (dd, $J = 15.65$, 8.90 Hz, 1 H), 6.68 (d, $J = 15.65$ Hz, 1 H), 7.76 (dd, $J = 8.59$, 1.84 Hz, 1 H), 8.08 (d, $J = 8.29$ Hz, 1 H), 8.18 (s, 1 H), 10.41 (s, 1 H), 13.04 (s, 1 H).

8-Bromo-2-((phenethylamino)methyl)[1]benzothieno[3,2-*d*]pyrimidin-4(3*H*)-one (21). The title compound was prepared using the same procedure as described for the synthesis of **19a**: ^1H NMR (400 MHz, DMSO- d_6) δ ppm 3.03–3.12 (m, 2 H), 3.40–3.47 (m, 2 H), 4.39 (s, 2 H), 7.27–7.34 (m, 3 H), 7.38 (t, $J = 7.48$ Hz, 2 H), 7.87 (dd, $J = 8.70$, 1.98 Hz, 1 H), 8.21 (d, $J = 8.54$ Hz, 1 H), 8.47 (d, $J = 2.14$ Hz, 1 H).

Pim Kinase Assays. Kinase assays were conducted as follows with final concentrations as listed. In 384-well v-bottom polypropylene plates, 10 μL of compound (2% DMSO) was mixed with 20 μL of Pim-1 (50 pM), Pim-2 (500 pM), or Pim-3 (300 pM) and peptide substrate (biotin- C_6 linker-VRRLRLTAREAA) (2 μM), followed by immediate initiation with 20 μL of λ -[^{33}P]-ATP (5 μM , 2mCi/ μmol) using a reaction buffer comprising 25 mM HEPES, pH 7.5, 0.5 mM DTT, 10 mM MgCl_2 , 100 μM Na_3VO_4 , and 0.075 mg/mL Triton X-100. Reactions were quenched after 1 h by the addition of 50 μL stop buffer (50 mM EDTA, 2 M NaCl). Eighty microliters of the stopped reactions were transferred to 384-well streptavidin-coated plates (Flash-Plate Plus, Perkin-Elmer), incubated 30 min at room temperature and washed three times with 0.05% Tween-20/PBS using an ELX-405 automated plate washer (BioTek) and counted on a TopCount Scintillation Plate Reader (Packard).

Selectivity Kinase Assays. Kinases were assayed using either radiometric or homogeneous time-resolved fluorescence (HTRF) in vitro kinase methods with the choice of format to provide maximal reagent efficiency. Radiometric assays were conducted exactly as described for the Pim in vitro assay except for the enzyme concentration and substrate used, which were custom to each kinase. Substrates were either chosen from those described in literature/vendor protocols or identified through screening of a 720 peptide Jerini kinase substrate set (Jerinin AG). HTRF assays were conducted using kinase-specific kinase concentration, ATP concentrations approximately 5-fold the respective ATP K_m , 0.5 μM biotinylated peptide substrate, 1 h reaction time, followed by addition of stop/detection buffer (30 mM EDTA, 1 $\mu\text{g/mL}$ streptavidin-APC (Prozyme), 50 ng/mL europium cryptate-conjugated phospho-specific monoclonal antibody (CisBio), 30 mM HEPES, pH 7.5, 120 mM KF, 0.005% Tween-20, 0.05% BSA). The antibody was PT66-K europium cryptate for tyrosine kinases or that from the Ser/Thr KinEase assay kit for Ser/Thr kinases. Quenched reactions were allowed to stand at room temperature for 1 h and then read in a time-resolved fluorescence detector (Envision, Perkin-Elmer) at 615 and 665 nm simultaneously. The ratio between the signal of 615 and 665 nm was used in the calculation of the IC_{50} . Serine kinases were assayed in 25 mM HEPES, pH 7.5, 0.5 mM DTT, 10 mM MgCl_2 , 100 μM Na_3VO_4 , 0.075 mg/mL Triton X-100, and 2% DMSO. Tyrosine kinases were assayed in 50 mM HEPES, pH 7.5, 10 mM MgCl_2 , 2 mM MnCl_2 , 0.1% BSA, 1 mM DTT, and 2% DMSO. Kinase-specific reagents (phosphotidyl serine, diacyl glycerol, calcium chloride, calmodulin, cGMP) were employed only where required.

Cell Viability Assays. K562 cells (ATCC, Manassas, VA) were cultured in Iscove's medium plus 10% fetal bovine serum (Invitrogen, Carlsbad, CA) and maintained at 37 $^\circ\text{C}$ (5% CO_2) in a humidified incubator. MV4-11 cells (ATCC, Manassas, VA) were cultured under the same conditions in RPMI + 10% fetal bovine serum (Invitrogen, Carlsbad, CA). Cells were seeded into 96-well tissue culture plates at 50 000 cells per well (100 μL medium per well), and compounds were then added at $2\times$ concentrations in 100 μL medium to give final concentrations ranging from 0.01 to 30 μM (half-log dilutions). The cells were incubated in the presence of compounds for 48 h at 37 $^\circ\text{C}$ (5% CO_2) and then analyzed by adding 20 μL alamarBlue reagent (Invitrogen, Carlsbad, CA) to each well and incubating until the reaction was complete, as

per manufacturer's instructions. Analysis was performed using an *fmax* fluorescence microplate reader (Molecular Devices, Sunnyvale, CA), set at the excitation wavelength of 544 nm and emission wavelength of 595 nm. Data were analyzed using SOFTmax PRO software provided by the manufacturer.

Effect of PIM inhibitors on the Bad Phosphorylation. Cells were treated with Pim inhibitors for 2 h and then scraped into cold PBS, pelleted, and then resuspended in 100–200 μL ice-cold insect cell lysis buffer supplemented with protease inhibitors. Cells were lysed by sonication, and the debris was cleared in a microcentrifuge. Forty micrograms of lysate was loaded in each well of 10% Tris-glycine polyacrylamide minigels for SDS-PAGE analysis. Proteins were transferred to PVDF membranes, blocked for 1 h in TBS-T plus 5% (w/v) powdered blotting grade milk, and then probed overnight at 4 $^\circ\text{C}$ with primary antibody (P-Bad antibody, S112 antibody from Cell Signaling Technology) at a 1:2000 dilution in blocking solution. Blots were developed using enhanced chemiluminescence (ECL Plus) reagents from Amersham Biosciences. P-Bad bands were scanned using a GS-800 densitometer to calculate the EC_{50} values.

X-ray Crystal Structure. Pim-1 ([Pim-1 (29-313)]-VD-6His) was expressed in *Escherichia coli*, purified, and crystallized using an adapted version of the method described by Kumar et al.⁴³ In brief, the protein was purified by nickel affinity, followed by ion exchange and finally size-exclusion chromatography. Protein ligand complexes were prepared by adding compound dissolved in DMSO (dimethyl sulfoxide) to the protein (18 mg/mL) to provide a final compound concentration of 1 mM. Crystallization plates (hanging drop vapor diffusion) were set using an equal volume of protein (18 mg/mL) and reservoir solution (0.4–0.9 M sodium acetate, 0.1 M imidazole pH 6.5) with the plate being incubated at 4 $^\circ\text{C}$. Crystals were cryo-cooled using 30% glycerol. Data were collected at APS, IMCA CAT BM-17, and the data were processed using HKL2000⁴⁴ and refined using Refmac.^{45–47} Crystals of **3b** diffracted to 2.1 \AA , with space group $P6_5$, $a = b = 96.8$, $c = 80.8$, and refined to an $R_{\text{work}} = 23.3\%$ and $R_{\text{free}} = 25.7\%$. Crystals of **6e** diffracted to 2.40 \AA , with space group $P6_5$, $a = b = 98.3$, $c = 80.6$, and refined to an $R_{\text{work}} = 22.8\%$ and $R_{\text{free}} = 26.2\%$. Crystals of **12b** diffracted to 2.8 \AA , with space group $P6_5$, $a = b = 96.8$, $c = 80.8$, and refined to an $R_{\text{work}} = 21.6\%$ and $R_{\text{free}} = 26.6\%$.

Acknowledgment. The authors thank Dr. Andrew Souers for critical reading of the manuscript, and Dr. Steven Elmore for support. The authors also wish to thank Dr. Michael Cohen for providing LaCaP-BAD cell line, the Department of Structural Chemistry for measuring NMR and MS spectra, the High-Through-Put Purification Group for analytical LC-MS, the Protein Biochemistry Group for the purification of Pim-1 protein used for X-ray crystallographic analysis, and the HT-ADME Group for the ADME profile of compound **14j**. The X-ray diffraction data were collected at beamline 17-BM in the facilities of the Industrial Macromolecular Crystallography Association Collaborative Access Team (IMCA-CAT) at the Advanced Photon Source. These facilities are supported by the companies of the Industrial Macromolecular Crystallography Association through a contract with Illinois Institute of Technology (IIT), executed through IIT's Center for Synchrotron Radiation Research and Instrumentation. Use of the Advanced Photon Source was supported by the U.S. Department of Energy, Basic Energy Sciences, Office of Science, under Contract No. W-31-109-Eng-38.

Note Added after ASAP Publication. This paper was published ASAP on October 16, 2009 with typographical errors. The revised version was published on October 20, 2009.

References

- (1) Cuypers, H. T.; Selten, G.; Quint, W.; Zijlstra, M.; Maandag, E. R.; Boelens, W.; van Wezenbeek, P.; Melief, C.; Berns, A. Murine leukemia virus-induced T-cell lymphomagenesis: Integration of proviruses in a distinct chromosomal region. *Cell* **1984**, *37*, 141–150.
- (2) Mikkers, H.; Allen, J.; Knipscheer, P.; Romeyn, L.; Hart, A.; Vink, E.; Berns, A. High-throughput retroviral tagging to identify components of specific signaling pathways in cancer. *Nat. Genet.* **2000**, *32*, 153–159.
- (3) van Lohuizen, M.; Verbeek, S.; Krimpenfort, P.; Domen, J.; Saris, C.; Radaszkiwicz, T.; Berns, A. Predisposition to lymphomagenesis in *pim-1* transgenic mice: Cooperation with *c-myc* and *N-myc* in murine leukemia virus-induced tumors. *Cell* **1989**, *56*, 673–682.
- (4) van Lohuizen, M.; Verbeek, S.; Scheijen, B.; Wientjens, E.; van der Gulden, H.; Berns, A. Identification of cooperating oncogenes in *Eμ-myc* transgenic mice by provirus tagging. *Cell* **1991**, *65*, 737–752.
- (5) van der Lugt, N. M. T.; Domen, J.; Verhoeven, E.; Linders, K.; van der Gulden, H.; Allen, J.; Berns, A. Proviral tagging in *Eμ-myc* transgenic mice lacking the *Pim-1* proto-oncogene leads to compensatory activation of *Pim-2*. *EMBO J.* **1995**, *14*, 2536–2544.
- (6) Mikkers, H.; Nawijn, M.; Allen, J.; Brouwers, C.; Verhoeven, E.; Jonkers, J.; Berns, A. Mice deficient for all Pim kinases display reduced body size and impaired responses to hematopoietic growth factors. *Mol. Cell. Biol.* **2004**, *24*, 6104–6115.
- (7) Lilly, M.; Sandholm, J.; Cooper, J. J.; Koskinen, P. J.; Kraft, A. The Pim-1 serine kinase prolongs survival and inhibits apoptosis-related mitochondrial dysfunction in part through a bcl-2-dependent pathway. *Oncogene* **1999**, *18*, 4022–4031.
- (8) Fox, C. J.; Hammerman, P. S.; Cinalli, R. M.; Master, S. R.; Chodosh, L. A.; Thompson, C. B. The serine/threonine kinase Pim-2 is a transcriptionally regulated apoptotic inhibitor. *Genes Dev.* **2003**, *17*, 1841–1854.
- (9) Yan, B.; Zemskova, M.; Holder, S.; Chin, V.; Kraft, A.; Koskinen, P. J.; Lilly, M. The Pim-2 kinase phosphorylates Bad on serine 112 and reverses Bad-induced cell death. *J. Biol. Chem.* **2003**, *278*, 45358–45367.
- (10) Macdonald, A.; Campbell, D. G.; Toth, R.; McLauchlan, H.; Hastie, C. J.; Arthur, J. S. Pim kinases phosphorylate multiple sites on Bad and promote 14-3-3 binding and dissociation from Bcl-XL. *BMC Cell Biol.* **2006**, *7*, 1.
- (11) Dhanasekaran, S. M.; Barrette, T. R.; Ghosh, D.; Shah, R.; Varambally, S.; Kurachi, K.; Pienta, K. J.; Rubin, M. A.; Chinnaiyan, A. M. Delineation of prognostic biomarkers in prostate cancer. *Nature* **2001**, *412*, 822–826.
- (12) Valdman, A.; Fang, X.; Pang, S. T.; Ekman, P.; Egevad, L. Pim-1 expression in prostatic intraepithelial neoplasia and human prostate cancer. *Prostate* **2004**, *60*, 367–371.
- (13) Xu, Y.; Zhang, T.; Tang, H.; Zhang, S.; Liu, M.; Ren, D.; Niu, Y. Overexpression of Pim-1 is a potential biomarker in prostate carcinoma. *J. Surg. Oncol.* **2005**, *92*, 326–330.
- (14) Kim, K. T.; Baird, K.; Ahn, J. Y.; Meltzer, P.; Lilly, M.; Levis, M.; Small, D. Pim-1 is up-regulated by constitutively activated FLT3 and plays a role in FLT3-mediated cell survival. *Blood* **2005**, *105*, 1759–1767.
- (15) Pasqualucci, L.; Neumeister, P.; Goossens, T.; Nanjangud, G.; Chaganti, R. S.; Kuppers, R.; Dalla-Favera, R. Hypermutation of multiple proto-oncogenes in B-cell diffuse large-cell lymphomas. *Nature* **2001**, *412*, 341–346.
- (16) Gaidano, G.; Pasqualucci, L.; Capello, D.; Berra, E.; Deambrogi, C.; Rossi, D.; Larocca, L. M.; Glohini, A.; Carbone, A.; Dalla-Favera, R. Aberrant somatic hypermutation in multiple subtypes of AIDS-associated non-Hodgkin lymphoma. *Blood* **2003**, *102*, 1833–1841.
- (17) Chen, W. W.; Chan, D. C.; Donald, C.; Lilly, M. B.; Kraft, A. S. Pim family kinases enhance tumor growth of prostate cancer cells. *Mol. Cancer Res.* **2003**, *3*, 443–451.
- (18) Dai, J. M.; Zhang, S. Q.; Zhang, W.; Lin, R. X.; Ji, Z. Z.; Wang, S. Q. Antisense oligodeoxynucleotides targeting the serine/threonine kinase Pim-2 inhibited proliferation of DU-145 cells. *Acta Pharmacol. Sinica* **2005**, *26*, 364–368.
- (19) Dai, H.; Li, R.; Wheeler, T.; Diaz de Vivar, A.; Frolov, A.; Tahir, S.; Agoulnik, I.; Thompson, T.; Rowley, D.; Ayala, G. Pim-2 upregulation: biological implications associated with disease progression and perineural invasion in prostate cancer. *Prostate* **2005**, *65*, 276–286.
- (20) For a review, see: Li, X.; Zhu, S.; Liu, L.; Huang, Y. Molecular characterization and biological effects of the Pim-3 gene. *Yixue Fenzi Shengwuxue Zazhi* **2008**, *5*, 146–148.
- (21) (a) Deneen, B.; Welford, S. M.; Ho, T.; Hernandez, F.; Kurland, I.; Denny, C. T. Pim3 proto-oncogene kinase is a common transcriptional target of divergent EWS/ETS oncoproteins. *Mol. Cell. Biol.* **2003**, *23*, 3897–3908. (b) Fujii, C.; Nakamoto, Y.; Lu, P.; Tsuneyama, K.; Popivanova, B. K.; Kaneko, S.; Mukaida, N. Aberrant expression of serine/threonine kinase Pim-3 in hepatocellular carcinoma development and its role in the proliferation of human hepatoma cell lines. *Int. J. Cancer* **2005**, *114*, 209–218. (c) Li, Y.-Y.; Popivanova, B. K.; Nagai, Y.; Ishikura, H.; Fujii, C.; Mukaida, N. Pim-3, a proto-oncogene with serine/threonine kinase activity, is aberrantly expressed in human pancreatic cancer and phosphorylates Bad to block Bad-mediated apoptosis in human pancreatic cancer cell lines. *Cancer Res.* **2006**, *66*, 6741–6747. (d) Popivanova, B. K.; Li, Y.-Y.; Zheng, H.; Omura, K.; Fujii, C.; Tsuneyama, K.; Mukaida, N. Proto-oncogene, Pim-3 with serine/threonine kinase activity, is aberrantly expressed in human colon cancer cells and can prevent Bad-mediated apoptosis. *Cancer Sci.* **2007**, *98*, 321–328.
- (22) Debreczeni, J. E.; Bullock, A. N.; Atilla, G. E.; Williams, D. S.; Bregman, H.; Knapp, S.; Meggers, E. Ruthenium half-sandwich complexes bound to protein kinase pim1. *Angew. Chem., Int. Ed.* **2006**, *45*, 1580–1585.
- (23) Bregman, H.; Meggers, E. Ruthenium half-sandwich complexes as protein kinase inhibitors: an *N*-succinimidyl ester for rapid derivatizations of the cyclopentadienyl moiety. *Org. Lett.* **2006**, *8*, 5465–5468.
- (24) Bullock, A. N.; Debreczeni, J. E.; Fedorov, O. Y.; Nelson, A.; Marsden, B. D.; Knapp, S. Structural basis of inhibitor specificity of the human protooncogene proviral insertion site in moloney murine leukemia virus (Pim-1) kinase. *J. Med. Chem.* **2005**, *48*, 7604–7614.
- (25) Pogacic, V.; Bullock, A. N.; Fedorov, O.; Filippakopoulos, P.; Gasser, C.; Biondi, A.; Meyer-Monard, S.; Knapp, S.; Schwaller, J. Structural analysis identifies imidazo[1,2-*b*]pyridazines as Pim kinase inhibitors with in vitro antileukemic activity. *Cancer Res.* **2007**, *67*, 6916–6924.
- (26) Bearss, D.; Liu, X.-H.; Grand, C.; Gourley, E.; Lamb, J.; Lloyd, M.; Vankayalapati, H. Discovery and characterization of a small molecule inhibitor for Pim-1 kinase. Abstract 414, American Society of Hematology National Meeting, **2006**.
- (27) (a) Lamb, J.; Gourley, E.; Liu, X.-H.; Grand, C.; Vankayalapati, H.; Warner, S.; Bearss, D. A small molecule inhibitor of Pim-1 kinase with activity in both hematological and solid tumor malignancies. Abstract 985, AACR-NCI-EORTC International Conference on Molecular Targets and Cancer Therapeutics, San Francisco, CA, **2007**. (b) Bearss, D. J.; Liu, X.-H.; Vankayalapati, H.; Xu, Y. Imidazo[1,2-*b*]pyridazine and pyrazolo[1,5-*a*]pyrimidine derivatives and their use as protein kinase inhibitors. WO 2008058126, **2005**.
- (28) Cheney, I. W.; Yan, S.; Appleby, T.; Walker, H.; Vo, T.; Yao, N.; Hamatake, R.; Hong, Z.; Wu, J. Z. Identification and structure–activity relationships of substituted pyridones as inhibitors of Pim1 kinase. *Bioorg. Med. Chem. Lett.* **2007**, *17*, 1679–1683.
- (29) Holder, S.; Lilly, M.; Brown, M. L. Comparative molecular field analysis of flavonoid inhibitors of the Pim-1 kinase. *Bioorg. Med. Chem.* **2007**, *15*, 6463–6473.
- (30) Holder, S.; Zemskova, M.; Zhang, C.; Tabrizizad, M.; Bremer, R.; Neidigh, J. W.; Lilly, M. B. Characterization of a potent and selective small-molecule inhibitor of the Pim1 kinase. *Mol. Cancer Ther.* **2007**, *6*, 163–172.
- (31) (a) Pierce, A. C.; Jacobs, M.; Stuver-Moody, C. Docking study yields four novel inhibitors of the protooncogene Pim-1 kinase. *J. Med. Chem.* **2008**, *51*, 1972–1975.
- (32) Tong, Y.; Stewart, K. D.; Thomas, S.; Przytulinska, M.; Johnson, E. F.; Klinghofer, V.; Levenson, J.; McCall, O.; Soni, N. B.; Luo, Y.; Lin, N.-H.; Sowin, T. J.; Giranda, V. L.; Penning, T. D. Isoxazolo[3,4-*b*]quinoline-3,4(1*H*,9*H*)-diones as unique, potent and selective inhibitors for Pim-1 and Pim-2 kinases: Chemistry, biological activities, and molecular modeling. *Bioorg. Med. Chem. Lett.* **2008**, *18*, 5206–5208.
- (33) Hammerman, P. S.; Fox, C. J.; Birnbaum, M. J.; Thompson, C. B. Pim and Akt oncogenes are independent regulators of hematopoietic cell growth and survival. *Blood* **2005**, *105*, 4477–4483.
- (34) Mizuki, M.; Schwable, J.; Steur, C.; Choudhary, C.; Agrawal, S.; Sargin, B.; Steffen, B.; Matsumura, I.; Kanakura, Y.; Böhrer, F. D.; Müller-Tidow, C.; Berdel, W. E.; Serve, H. Suppression of myeloid transcription factors and induction of STAT response genes by AML-specific Flt3 mutations. *Blood* **2003**, *101*, 3164–3173.
- (35) Adam, M.; Pogacic, V.; Bendit, M.; Chappuis, R.; Nawijn, M. C.; Duyster, J.; Fox, C. J.; Thompson, C. J.; Cools, J.; Schwaller, J. Targeting Pim kinases impairs survival of hematopoietic cells transformed by kinase inhibitor-sensitive and kinase inhibitor-resistant forms of Fms-like tyrosine kinase 3 and BCR/ABL. *Cancer Res.* **2006**, *66*, 3828–3835.

- (36) (a) Xia, Z.; Knaak, C.; Ma, J.; Beharry, Z. M.; McInnes, C.; Wang, W.; Kraft, A. S.; Smith, C. D. Synthesis and evaluation of novel inhibitors of Pim-1 and Pim-2 protein kinases. *J. Med. Chem.* **2009**, *52*, 74–86. (b) Qian, K.; Wang, L.; Cywin, C. L.; Farmer, B. T.; Hickey, E.; Homon, C.; Jakes, S.; Kashem, M. A.; Lee, G.; Leonard, S.; Li, J.; Magboo, R.; Wang, M.; Pack, E.; Peng, C.; Prokopowicz, A.; Welzel, M.; Wolak, J.; Morwick, T. Hit to lead account of the discovery of a new class of inhibitors of Pim kinases and crystallographic studies revealing an unusual kinase binding mode. *J. Med. Chem.* **2009**, *52*, 1814–1827.
- (37) (a) Robba, M.; Touzot, P.; Riquelme, R. M. Synthèse de benzo(1)-thieno[2,3-*d*]pyrimidines et de benzo(1)thieno[3,2-*d*]pyrimidines. *Tetrahedron Lett.* **1972**, *44*, 4549–4551. (b) Robba, M.; Touzot, P.; El-Kashef, H. [1]Benzothienopyrimidines. I. Etude de la 3H-benzothieno[3,2-*d*]pyrimidone-4. *J. Heterocycl. Chem.* **1980**, *17*, 923–928. (c) Bridges, A. J.; Zhou, H. Synthetic methodology for the preparation of benzo[b]thieno[3,2-*d*]pyrimidines substituted with electron donating substituents on the benzene ring. *J. Heterocycl. Chem.* **1997**, *34*, 1134–1139. (d) Showalter, H. D. H.; Bridges, A. J.; Zhou, H.; Sercel, A. D.; McMichael, A.; Fry, D. W. Tyrosine kinase inhibitors. 16. 6,5,6-Tricyclic benzothieno[3,2-*d*]pyrimidines and pyrimido[5,4-*b*] and -[4,5-*b*]indoles as potent inhibitors of the epidermal growth factor receptor tyrosine kinase. *J. Med. Chem.* **1999**, *42*, 1814–1827.
- (38) (a) Qian, K. C.; Wang, L.; Hickey, E. R.; Studts, J.; Barringer, K.; Peng, C.; Kronkatis, A.; Li, J.; White, A.; Mische, S.; Farmer, B. Structural basis of constitutive activity and a unique nucleotide binding mode of human Pim-1 kinase. *J. Biol. Chem.* **2005**, *280*, 6130–6137. (b) Jacobs, M. D.; Black, J.; Futer, O.; Swenson, L.; Hare, B.; Fleming, M.; Saxena, K. Pim-1 ligand-bound structures reveal the mechanism of serine/threonine kinase inhibition by LY294002. *J. Biol. Chem.* **2005**, *280*, 13728–13734. (c) Kumar, A.; Mandiyan, V.; Suzuki, Y.; Zhang, C.; Rice, J.; Tsai, J.; Artis, D. R.; Ibrahim, P.; Bremer, R. Crystal structures of proto-oncogene kinase Pim1: A target of aberrant somatic hypermutations in diffuse large cell lymphoma. *J. Mol. Biol.* **2005**, *348*, 183–193. (d) Bullock, A. N.; Debreczeni, J. E.; Amos, A. L.; Knapp, S.; Turk, B. E. Structure and substrate specificity of the Pim-1 kinase. *J. Biol. Chem.* **2005**, *280*, 41675–41682.
- (39) Knight, Z. A.; Shokat, K. M. Features of selective kinase inhibitors. *Chem. Biol.* **2005**, *12*, 621–637.
- (40) (a) Tao, Z.-F.; Wang, L.; Stewart, K. D.; Chen, Z.; Gu, W.; Bui, M.; Merta, P.; Zhang, H.; Kovar, P.; Johnson, E.; Park, C.; Judge, R.; Rosenberg, S.; Sowin, T.; Lin, N.-H. Structure-based design, synthesis, and biological evaluation of potent and selective macrocyclic checkpoint kinase 1 inhibitors. *J. Med. Chem.* **2007**, *50*, 1514–1527. (b) Wendt, M. D.; Shen, W.; Kunzer, A.; McClellan, W. J.; Bruncko, M.; Oost, T. K.; Ding, H.; Joseph, M. K.; Zhang, H.; Nimmer, P. M.; Ng, S.-C.; Shoemaker, A. R.; Petros, A. M.; Oleksijew, A.; Marsh, K.; Bauch, J.; Oltersdorf, T.; Belli, B. A.; Martineau, D.; Fesik, S. W.; Rosenberg, S. H.; Elmore, S. W. Discovery and structure–activity relationship of antagonists of B-cell lymphoma 2 family proteins with chemopotential activity in vitro and in vivo. *J. Med. Chem.* **2006**, *49*, 1165–1181. (c) Bruncko, M.; Oost, T. K.; Belli, B. A.; Ding, H.; Joseph, M. K.; Kunzer, A.; Martineau, D.; McClellan, W. J.; Mitten, M.; Ng, S.; Nimmer, P. M.; Oltersdorf, T.; Park, C.-M.; Petros, A.; Shoemaker, A. R.; Song, X.; Wang, X.; Wendt, M. D.; Zhang, C.; Fesik, S. W.; Rosenberg, S.; Elmore, S. W. Studies leading to potent, dual inhibitors of Bcl-2 and Bcl-xL. *J. Med. Chem.* **2007**, *50*, 641–662. (d) Zhu, G. D.; Gandhi, V. B.; Gong, J.; Thomas, S.; Woods, K. W.; Song, X.; Li, T.; Diebold, R. B.; Luo, Y.; Liu, X.; Guan, R.; Klinghofer, V.; Johnson, E. F.; Bouska, J.; Olson, A.; Marsh, K. C.; Stoll, V. S.; Mamo, M.; Polakowski, J.; Campbell, T. J.; Martin, R. L.; Gintant, G. A.; Penning, T. D.; Li, Q.; Rosenberg, S. H.; Giranda, V. L. Syntheses of potent, selective, and orally bioavailable indazole-pyridine series of protein kinase B/Akt inhibitors with reduced hypotension. *J. Med. Chem.* **2007**, *50*, 2990–3003. (e) Park, C.-M.; Bruncko, M.; Adickes, J.; Bauch, J.; Ding, H.; Kunzer, A.; Marsh, K. C.; Nimmer, P.; Shoemaker, A. R.; Song, X.; Tahir, S. K.; Tse, C.; Wang, X.; Wendt, M. D.; Yang, X.; Zhang, H.; Fesik, S. W.; Rosenberg, S. H.; Elmore, S. W. Discovery of an orally bioavailable small molecule inhibitor of prosurvival B-cell lymphoma 2 proteins. *J. Med. Chem.* **2008**, *51*, 6902–6915.
- (41) Taghiyev, A. F.; Guseva, N. V.; Harada, H.; Knudson, C. M.; Rokhlin, O. W.; Cohen, M. B. Overexpression of Bad potentiates sensitivity to tumor necrosis factor-related apoptosis-inducing ligand treatment in the prostatic carcinoma cell line LNCaP. *Mol. Cancer Res.* **2003**, *1*, 500–507.
- (42) Pim kinases have emerged as a potential target in immunology: (a) Aho, T. L. T.; Lund, R. J.; Ylikoski, E. K.; Matikainen, S.; Lahesmaa, R.; Koskinen, P. J. Expression of human pim family genes is selectively up-regulated by cytokines promoting T helper type 1, but not T helper type 2, cell differentiation. *Immunology* **2005**, *116*, 82–88. (b) Li, J.; Peet, G. W.; Balzarano, D.; Li, X.; Massa, P.; Barton, R. W.; Marcu, K. B. Novel NEMO/I κ B kinase and NF- κ B target genes at the pre-B to immature B cell transition. *J. Biol. Chem.* **2001**, *276*, 18579–18590. (c) Rainio, E.; Sandholm, J.; Koskinen, P. J. Cutting edge: transcriptional activity of NFATc1 is enhanced by the Pim-1 kinase. *J. Immunol.* **2002**, *168*, 1524–1527. (d) Zhu, N.; Ramirez, L. M.; Lee, R. L.; Magnuson, N. S.; Bishop, G. A.; Gold, M. R. CD40 signaling in B cells regulates the expression of the Pim-1 kinase via the NF- κ B pathway. *J. Immunol.* **2002**, *168*, 744–754. (e) Fox, C. J.; Hammerman, P. S.; Thompson, C. B. The Pim kinases control rapamycin-resistant T cell survival and activation. *J. Exp. Med.* **2005**, *201*, 259–266.
- (43) Kumar, A.; Mandiyan, V.; Suzuki, Y.; Zhang, C.; Rice, J.; Tsai, J.; Artis, D. R.; Ibrahim, P.; Bremer, R. Crystal structures of proto-oncogene kinase Pim-1: A target of aberrant somatic hypermutations in diffuse large cell lymphoma. *J. Mol. Biol.* **2005**, *348*, 183–193.
- (44) Otwinowski, Z.; Minor, W. In *Methods in Enzymology, Macromolecular Crystallography, Part A*; Carter, C. W., Jr., Sweet, R. M., Eds.; Academic Press: New York, 1997; Vol. 276, pp 307–326.
- (45) Murshudov, G.; Vagin, A.; Dodson, E. Application of maximum likelihood refinement in the refinement of protein structures. *Proc. Daresbury Study Weekend* **1996**.
- (46) Murshudov, G. N.; Vagin, A.; Dodson, E. J. Refinement of macromolecular structures by the maximum-likelihood method. *Acta Crystallogr., Sect. D* **1997**, *D53*, 240–255.
- (47) Pannu, N. J.; Murshudov, G. N.; Dodson, E. J.; Read, R. J. Incorporation of prior phase information strengthens maximum-likelihood structure refinement. *Acta Crystallogr., Sect. D* **1998**, *D54*, 1285–1294.